



УНИВЕРЗИТЕТ У НОВОМ САДУ  
ГРАЂЕВИНСКИ ФАКУЛТЕТ СУБОТИЦА

24000 Суботица, Козарачка 2а, www.gf.uns.ac.rs, dekanat@gf.uns.ac.rs  
Тел: (024) 554-300, Факс: (024) 554-580, ТР: 840-1233666-68, ПИБ: 100843783



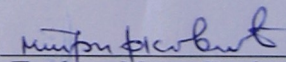
Дел. број:  
Датум:

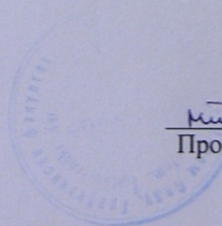
278-1  
26. 4. 2024.

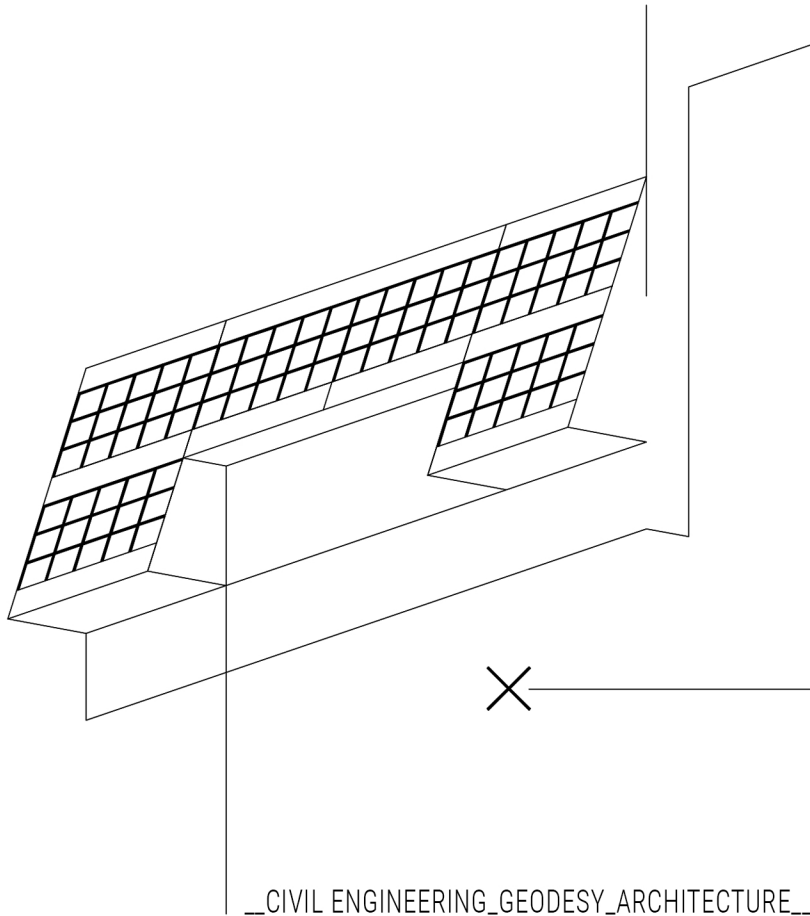
## ПОТВРДА

Овим потврђујемо да је ванредни професор др Дејана Ђорђевић, одржала предавање по позиву на 9. међународној конференцији „Савремена достигнућа у грађевинарству 2024“, одржаној 25-26. априла 2024. године у Суботици. Наслов саопштеног предавања је: „ON THE APPLICATION OF THE DOUBLE-AVERAGING METHODOLOGY IN MODELLING VEGETATED OPEN-CHANNEL FLOWS“.

Декан

  
Проф. др Милан Трифковић





**IX** INTERNATIONAL CONFERENCE  
CONTEMPORARY ACHIEVEMENTS IN CIVIL ENGINEERING  
**CONFERENCE PROCEEDINGS**

ISBN 978-86-80297-98-9

**IX INTERNATIONAL CONFERENCE  
CONTEMPORARY ACHIEVEMENTS IN  
CIVIL ENGINEERING**

**CONFERENCE PROCEEDINGS**

SUBOTICA 2024



UNIVERSITY OF NOVI SAD  
FACULTY OF CIVIL ENGINEERING SUBOTICA

For the publisher:	Prof. dr Milan TRIFKOVIĆ, Dean
Editors:	Prof. dr Vukan OGRIZOVIĆ Doc. dr Smilja BURSACĆ Doc. dr Jelena TATALOVIĆ
Organizing Committee:	Doc. dr Smilja BURSACĆ Doc. dr Olivera DULIĆ Doc. dr Milena GRBIĆ Doc. dr Dušan JOVANOVIĆ Prof. dr Ljiljana KOZARIĆ Prof. dr Vukan OGRIZOVIĆ Milica PAVIĆ Ramona PETROV Doc. dr Mila SVILAR Doc. dr Jelena TATALOVIĆ Prof. dr Martina VOJNIĆ PURČAR
Technical processing:	Doc. dr Smilja BURSACĆ Doc. dr Milena GRBIĆ Milica PAVIĆ Ramona PETROV
Publisher	University of Novi Sad, Faculty of Civil Engineering Subotica Kozaračka 2a, 24000 Subotica, Serbia URL: <a href="http://conference.gf.uns.ac.rs">conference.gf.uns.ac.rs</a> e-mail: <a href="mailto:konferencija@gf.uns.ac.rs">konferencija@gf.uns.ac.rs</a>
Book circulation:	200 copies
ISBN:	978-86-80297-98-9
Print:	Birografika MB, Subotica

## Scientific Committee

Dr Biljana Antunović, University of Banja Luka, Faculty of Architecture, Civil Engineering and Surveying

Dr Teodor Atanacković, SANU

Dr Gyorgy Balazs, Budapest University of Technology and Economics

Dr Meri Cvetkovska, University "St. Cyril and Methodius", Faculty of Civil Engineering

Dr Saša Čvoro, University of Banja Luka, Faculty of Architecture, Civil Engineering and Surveying

Dr Domagoj Damjanović, University of Zagreb

Dr Radomir Folić, University of Novi Sad, Faculty of Technical Sciences

Dr Jovo Jarić, University of Belgrade, Faculty of Mathematics

Dr Vojkan Jovičić, University of Ljubljana

Dr Miloš Knežević, University of Montenegro, Faculty of Civil Engineering

Dr Miloš Kojić, SANU

Dr Srđan Kolaković, University of Novi Sad, Faculty of Technical Sciences

Dr Hrvoje Krstić, Josip Juraj Strossmayer University in Osijek

Dr Nađa Kurtović-Folić, University of Novi Sad, Faculty of Technical Sciences

Dr Vladan Kuzmanović, University of Belgrade, Faculty of Civil Engineering

Dr Duško Lučić, University of Montenegro, Faculty of Civil Engineering

Dr Goran Markovski, University "St. Cyril and Methodius", Faculty of Civil Engineering

Dr Siniša Mesarović, Washington State University, School of Mechanical and Materials Engineering

Dr Jasna Plavšić, University of Belgrade, Faculty of Civil Engineering

Dr Dušan Prodanović, University of Belgrade, Faculty of Civil Engineering

Dr Marina Rakočević, University of Montenegro, Faculty of Civil Engineering

Dr Dragoslav Šumarac, University of Belgrade, Faculty of Civil Engineering

Dr Slaviša Trajković, University of Niš

Dr Rade Vignjević, Brunel University

Dr Aleksandar Sedmak, University of Belgrade, Faculty of Mechanical Engineering

Dr Boris Podreka, SANU

Dr Mladen Zrinjski, University of Zagreb, Faculty of Geodesy

Dr Dragan Kuzmanović, University of Belgrade, Faculty of Transport and Traffic Engineering

Dr Goran Šimunović, University of Slavonski Brod, Mechanical engineering Faculty

Dr János Major, University of Debrecen, Faculty of Engineering

The International Conference on Contemporary Achievements in Civil Engineering, taking place in Subotica, Serbia, from April 25 to 26, 2024, is set to explore the latest innovations and forward-thinking ideas in civil engineering, architecture, and geodesy. This ninth edition of the conference is a platform for experts to share research, designs, and practices that push the boundaries of the field, offering a glimpse into the future of civil engineering.

The conference significantly contributes to the scientific community by serving as a forum for the presentation and discussion of the latest research, innovations, and practices within civil engineering and corresponding fields. It emphasizes the exchange of knowledge and ideas that foster scientific advancement and the application of new technologies and methodologies in the field, thereby playing a crucial role in shaping the future of civil engineering disciplines.

This year's conference is particularly momentous as it coincides with the 50th anniversary of the Faculty of Civil Engineering in Subotica. This landmark occasion not only celebrates half a century of academic and professional excellence but also reflects on the significant contributions the faculty has made to the field of civil engineering. The conference, in this celebratory year, stands as a testament to the faculty's enduring legacy and its commitment to advancing civil engineering.

Therefore, we wish to thank all the authors who have submitted their papers. Your contributions are invaluable to the scientific community and the success of this conference. Your research, insights, and dedication to advancing civil engineering, architecture, and geodesy help pave the way for future innovations and achievements. We are grateful for your participation and look forward to your continued engagement with our community.

Organizing Committee





## CONTENTS

### I INVITED PAPER

**Boris Folić, Miloš Čokić, Radomir Folić**

RESPONSE SPECTRA OF RECORDING OF VRANCEA EARTHQUAKES OF 1977 AND 1986  
.....3

**Nataša Živaljević Luxor, Nadja Kurtović Folić**

IMMOVABLE CULTURAL GOODS IN THE CONTEXT OF ECONOMIC SELF-  
SUSTAINABILITY – A CASE STUDY OF THE FORTRESS IN NIŠ .....20

**Dejana Đorđević**

ON THE APPLICATION OF THE DOUBLE-AVERAGING METHODOLOGY IN MODELLING  
VEGETATED OPEN-CHANNEL FLOWS .....29

**Žikica Tekić**

DESIGN OF TIMBER STRUCTURES IN THE LKV SYSTEM .....64

**Siniša Delčev, Olivera Vasović Šimšić, Jelena Gučević**

APPLICATION OF UNMANNED AERIAL VEHICLES FOR LEGALIZATION OF BUILDINGS 65

### II CIVIL ENGINEERING

**Milan Bursać, Svetlana M. Kostić**

PLASTIC BENDING RESISTANCE OF COMPOSITE BEAMS ACCORDING TO SECOND  
GENERATION EUROCODE 4 .....77

**Dragan D. Milašinović, Smilja Bursać, Nataša Mrđa Bošnjak, Arpad Čeh**

CRITICAL VOID VOLUME FRACTION OF CONCRETE .....86

**Dragan D. Milašinović, Smilja Bursać, Aleksandar Pančić**

MODELLING OF POROUS METALS BY RDA-PT MODEL .....99

**Ilija M. Miličić, Ivana I. Miličić, Aleksandar D. Prokić**

FFT ANALYSIS AND FILTERING OF OSCILLATING RESPONSE SIGNALS OF A SIMPLE  
WOOD GIRDER IN A VERTICAL PLANE .....118

**Petar Knežević, Dragan Čukanović, Zoran Perović, Aleksandar Radaković, Nikola  
Velimirović**

CYCLIC BEHAVIOR PHENOMENA OF STRUCTURAL STEEL .....131

**Petar Praštalo, Anica Milanović, Dušan Prodanović**

LOW-COST RAINWATER RUNOFF MEASUREMENT DEVICE .....140

**Ilija M. Miličić, Ivana I. Miličić, Radomir J. Folić**

DFT ANALYSIS OF VERTICAL DISPLACEMENT SIGNALS OF A SIMPLE WOOD GIRDER BY MONITORING USING SENSORS VL6180X..... 150

**Branislav Vuković, Ivana Perčić, Danica Goleš**

REHABILITATION AND RECONSTRUCTION OF THE UNDERGROUND PUMP STATION "RAILWAY STATION" ON THE SAVA SQUARE IN BELGRADE ..... 167

**Svjetlana Banjac, Zoran Mitrović**

APPLICATION OF PEARSON'S CORRELATION COEFFICIENT IN THE ANALYSIS OF CONCRETE SAMPLES..... 187

**Todor Vacev, Danijela Đurić Mijović, Andrija Zorić**

COMPARATIVE ANALYSIS OF WIND ACTION ON CONTAINER STACKS ANALYTICALLY AND BY FEM CONTACT ANALYSIS ..... 196

**mr Mihailo Ostojić, dr Milivoje Rogac**

INTEGRATION OF VIRTUAL MODELS AND PHYSICAL CONSTRUCTION - CYBER PHYSICAL SYSTEMS (CPS) IN THE ARCHITECTURAL, CIVIL/CONSTRUCTION & TRANSPORTATION ENGINEERING INDUSTRIES (ACCTEI)..... 209

**Zoran Spajić, Igor Jokanović, Milica Pavić**

CONNECTION OF INTERCITY AND URBAN ROADS: CASE STUDY KULA, EAST SARAJEVO ..... 219

**Stanković Natalija**

THE ROLE OF THE URBAN GREEN INFRASTRUCTURE CONCEPT IN STORMWATER MANAGEMENT ..... 234

**Andrija Zorić, Miloš Milić, Marina Trajković-Milenković, Todor Vacev, Ivana Nešović, Katarina Slavković**

SEMI-ANALYTICAL SOLUTION FOR ELASTO-PLASTIC DEFLECTION OF PRISMATIC SIMPLY SUPPORTED BEAMS WITH CIRCULAR CROSS-SECTION ..... 244

**Ivana Perčić, Arpad Čeh, Danica Goleš**

THE INFLUENCE OF BASALT FIBERS ON THE COMPRESSIVE AND FLEXURAL STRENGTH OF LIGHTWEIGHT CONCRETE ..... 257

**Miloš Milić, Todor Vacev, Ivan Nešović, Predrag Petronijević, Andrija Zorić, Radovan Perić**

DEVELOPMENT OF A STEEL-TIMBER COMPOSITE CONNECTOR ..... 269

**Đorđe Marković, Bojan Milovanović, Aleksandar Savić, Vladan Kuzmanović, Ljubodrag Savić**

USE OF CONCRETE WITH FLY ASH FOR CONSTRUCTION RETENTION DAMS .....280

**Milan Kekanović, Danica Goleš, Ljilja Kozarić, Matija Benčik, Hilda Horvat, Nikola Milosavljević**

EXPERIMENTAL-THEORETICAL ANALYSIS OF VERIFYING THE CURRENT PROCEDURE AND FINDING THE CORRECT PROCEDURE AND METHODS FOR TESTING COMPRESSIVE STRENGTH OF ORDINARY CONCRETE .....290

**Ivana Mitrović, Žarko Nestorović**

GROUND WATER LEVEL IN LARGE DAMS' BASINS MODELING .....303

**Ildiko Molnar, Janos Major, Milan Kekanovic, Viktor Fabian, Erik Heđi, Mihajlo Mirosavljević**

RESEARCH OF CHARACTERISTICS OF OIL-RESISTANT CONCRETES WITH ADDITIVES 309

S.G. Emelyanov, A.V. Brezhnev, A.I. Pykhtin, N.E. Semicheva

MONITORING BIM MODELS IN VIRTUAL AND AUGMENTED REALITY (VR/AR).....323

**Milan Kekanović, Dragoslav Šumarac , Milan Trifković, Miroslav Kuburić, Stanko Ćorić, Arpad Čeh, Žarko Nestorović**

THERMODYNAMIC APPROACH TO ISOLATION OF RESIDENTIAL BUILDINGS - BUILDINGS WITHOUT THERMAL BRIDGES .....328

**Vladislav Pakhomov, Ekaterina Pakhomova, Natalia Semicheva**

WAYS TO REDUCE THE IMPACT OF HARMFUL EMISSIONS FROM BOILERS AND VEHICLES ON THE ENVIRONMENT .....357

**Artem Brezhnev, Elvira Aleksapolskaya, Natalia Semicheva**

METHODS FOR DETECTING COLLISIONS AND ERRORS USING BIM TECHNOLOGIES IN THE DESIGN OF HEATING, VENTILATION AND AIR CONDITIONING SYSTEMS OF HIGH-RISE BUILDINGS .....364

**Jovana Topalić, Tiana Milović, Vladimir Mučenski**

THE POTENTIAL OF NATURAL ZEOLITE USE IN INDUSTRIAL WASTEWATER TREATMENT .....370

**Milovan Bjelica, Vladimir Zotović**

MODELS FOR HYDROPOWER PRODUCTION ANALYSIS .....380

**Iva Despotović, Nemanja Bralović**

TOWARDS THE NEW GENERATION OF EUROCODE 7.....386

**Ksenija Janković, Srboljub Stanković**

NEUTRON SHIELDING PARAMETERS OF SELECTED TYPES OF CONCRETE ..... 396

**Mila Svilar, Igor Peško, Ramona Petrov, Nikola Banjac**

ESTIMATION OF HIGHWAY CONSTRUCTION COSTS USING MACHINE LEARNING ... 405

**III ARCHITECTURE**

**Vasilevska Ljiljana, Živković Jelena, Slavković Magdalena**

URBAN TRANSFORMATIONS AND PLANNING STRATEGIES FOR DEVELOPMENT OF  
LARGE HOUSING ESTATES IN THE POST-SOCIALIST CONTEXT: THE EXPERIENCE OF  
THE BALTIC COUNTRIES ..... 421

**Lilia Tchaikovskaya, Ekaterina Pakhomova, Aleksei Shleenko**

MODELING OF "ENTERTAINMENT AND EMOTIONS" CITY FUNCTION ..... 435

**Milos Nedeljko, Miomir Vasov, Dragan Kostic, Dusan Randjelovic, Vuk Milosevic**

UNLOCKING THE BENEFITS OF ENERGY RENOVATION IN BUILDINGS: CORRELATING  
REGULATIONS ACROSS REGIONAL COUNTRIES ..... 442

**Aleksandra Cilić, Jelena Savić, Danijela Đurić-Mijović, Maša Ranđelović, Jelena  
Stevanović**

POSSIBILITIES OF USING OLD SHIPPING CONTAINERS AS MODULAR UNITS IN A  
CELLULAR SYSTEM FOR THE CONSTRUCTION OF MULTI-STOREY APARTMENT  
BUILDINGS ..... 453

**Dušan Stajić, Ana Momčilović Petronijević, Ivana Cvetković, Mirko Stanimirović**

DEGRADATION OF THE IDENTITY OF URBAN STRUCTURES BY INTENSIVE  
CONSTRUCTION ..... 464

**Relja Petrović**

THE USE OF ARTIFICIAL INTELLIGENCE AS A METHODOLOGICAL TOOL IN  
INTERPRETING SPATIAL SENSATIONS ..... 479

**Milena Grbić**

THE PHANTASMAGORIA OF DRAWINGS AS A METHODOLOGICAL OUTLINE OF  
DESIGN ..... 485

**Bogdan Krmpot, Branislava Stoiljković**

CONCEPTUAL SOLUTION OF TERRACED HOUSES IN NIŠ ..... 496

**Monika Štiklica**

ANALYSIS OF APPLIED DESIGN STRATEGY IN A CONSTRUCTED FAMILY VILLA: A CASE  
STUDY ..... 507

**Jelena Savić, Danijela Đurić Mijović, Aleksandra Cilić, Danijela Milanović, Miloš Nedeljković**

POSSIBILITIES IN TRANSFORMATION THE FACADES OF EXISTING DILAPIDATED BUILDINGS - A DIALOGUE OF EPOCHS .....523

**Stefan Škorić, Ph.D., Dijana Brkljač, Ph.D. prof. Aleksandra Milinković, prof. Milena Krklješ, Ph.**

INFLUENCE OF SPATIAL ARRANGEMENT OF OPEN PUBLIC SPACES ON PEDESTRIAN MOBILITY AND ACTIVITIES .....533

**Dr. Tatjana Babić, Dr. Milena Krklješ**

EMERGENCE, DEVELOPMENT, AND TRANSFORMATION OF VILLA ZONES IN NOVI SAD DURING THE 20TH CENTURY .....544

**Olivera Dulić**

THEMATIC CONTENT ANALYSIS OF INTRODUCTORY ARCHITECTURAL STUDIO COURSES IN THE REPUBLIC OF SERBIA.....559

**Aleksandar Kostić, Katarina Krstić, Dušan Turina, Nikola Simić**

DIDACTIC APPROACH TO AUTODESK REVIT TRAINING COURSE .....569

**Ivan Stevović, Jovana Jovanović, Sabahudin Hadrović**

GREEN BUILDINGS, ENERGY EFFICIENCY AND RAISING AWARENESS ABOUT ENVIRONMENTAL PROTECTION .....576

**Ivan Stevović, Jovana Jovanović, Mihailo Jovanović**

ARTIFICIAL INTELLIGENCE METHODS ON SUSTAINABLE PATH IN THE FUNCTION OF ENERGY EFFICIENCY INCREASE.....585

**IV GEODESY**

**Marina Davidović Manojlović, Gordana Nataroš**

THE FLOW OF CONFISCATION AND RESTITUTION OF LAND .....595

**Antonio Tupek, Mladen Zrinjski, Đuro Barković, Krunoslav Špoljar**

ABSOLUTE GNSS RECEIVER ANTENNA CALIBRATION AT THE FACULTY OF GEODESY - UNIVERSITY OF ZAGREB .....604

**Maja Đorđević Radulović, Danijela Radosavljević, Andriana Bekerević, Evica Šejnjanović, Žarko Nestorović**

GEODETIC MEASSUREMENTS ACCURACY UNDER DIFFERENT LEVEL OF LIGHT .....617

**Gordana Nataroš, Milorad Vučković, Milan Trifković**

COMPACTION AND ARRONDATION ON THE TERRITORY OF SERBIA .....626

**Stefan Istodorović, Žarko Nestorović**

PENDULUM MOVEMENT ON LARGE DAM DEPENDENCES ON OUTER INFLUENCES 634

**Marko Z. Marković, Mehmed Batilović, Đuro Krnić, Marijana Vujinović, Zoran Sušić**

APPLICATION OF TERRESTRIAL LASER SCANNING TECHNOLOGY IN THE ANALYSIS OF  
THE COLUMNS VERTICALITY AND THE CREATION OF A 3D MODEL OF THE SPORTS  
HALL ..... 640

**Ivana Racetin, Robert Župan**

CONTEMPORARY USERS OF STOKIS TOPOGRAPHIC AND CARTOGRAPHIC DATA .... 653

**Dragan Kostić, Milorad Zlatanović, Miomir Vasov, Miloš Nedeljković, Srđan Aleksić**

MARKET VALUE ASSESSMENT OF CADASTRAL PARCELS USING HIGH-AND-BEST-USE  
ANALYSIS AND YIELD APPROACH..... 662

**Marijana Vujinović, Vladimir Bulatović, Marko Z. Marković, Mehmed Batilović, Đuro  
Krnić**

TERRESTRIAL REFERENCE FRAMES: FOUNDATION FOR POSITIONING AND EARTH  
SCIENCES..... 675

**Marinković Goran, Ilić Zoran, Nestorović Žarko**

MODEL FOR RISK MANAGEMENT IN LAND CONSOLIDATION PROJECTS REALIZATION  
..... 686

**Jelena Tatalović, Milan Trifković, Bogdan Bojović**

THE ROLE AND SIGNIFICANCE OF LAND CONSOLIDATION PROJECTS ON THE  
SUSTAINABLE DEVELOPMENT OF THE AREA. CASE STUDY: THE MUNICIPALITY OF  
BAČKA TOPOLA ..... 693

**Milan Trifković, Miroslav Kuburić, Žarko Nestorović**

PARADOXES OF REGRESSION MODELS ..... 701

***I INVITED PAPERS***

# ON THE APPLICATION OF THE DOUBLE-AVERAGING METHODOLOGY IN MODELLING VEGETATED OPEN-CHANNEL FLOWS

Dejana Đorđević<sup>1\*</sup>

<sup>1</sup> University of Belgrade, Faculty of Civil Engineering, Belgrade, Serbia

\* corresponding author: dejana@grf.bg.ac.rs

UDK: 532.51:519.6  
DOI: 10.14415/CACE2024.03  
CC-BY-SA 4.0 licence

## ABSTRACT

The double-averaging methodology (DAM) arose to respond to a need to provide a mathematically rigorous tool for describing spatially heterogeneous turbulent flows. Initial developments originate from micrometeorologists who revealed notable discrepancies between measured and simulated temperature and moisture fields above trees when using only Reynolds-averaged Navier-Stokes (RANS) equations with various turbulence model closures. The discrepancies were attributed to the spatial inhomogeneity of the flow field caused by vegetation. Thus, additional spatial averaging of RANS equations over horizontal planes sufficiently large to provide statistical averaging of all differences caused by an arbitrary distribution of plants and the influence of the biggest vortices responsible for the transfer of momentum was suggested. The advantages of using the DAM in open-channel hydraulics of gravel-bed rivers were recognised in the early 2000s when DAM was first applied and consequently improved. Open-channel vegetated flows are another example of spatially heterogeneous turbulent flows to which the DAM can be applied. The paper presents the results of the DoubleVeg project led by the author, in which a new set of equations was derived. After introducing the basic DAM concepts, the procedure of deriving Depth-Integrated Double-Averaged Navier-Stokes equations is presented. Consequently, the main challenges in solving these equations are discussed, and the results of initial testing of systems of homogeneous and non-homogeneous equations are shown.

## KEYWORDS:

SPATIALLY HETEROGENEOUS FLOWS, REPRESENTATIVE AVERAGING VOLUME, POROSITY, DOUBLE AVERAGING, DIDANS EQUATIONS, ADAPTED ROE'S METHOD



## 1 INTRODUCTION

This paper aims to introduce the scientific community in the Balkans to the Double Averaging Methodology (DAM) and the advantages it provides when applied in open-channel hydraulics. The DAM combines time averaging for modelling turbulent flows with spatial averaging for modelling laminar flows in a porous medium. Reynolds proposed time averaging of instantaneous flow variables in the mid-19th century to facilitate analysis of turbulent flows (Figure 1a – averaging along the  $t$ -axis for each member of the ensemble). His original idea was modified in the late 1930ies with the averaging over the set (ensemble) of statistically random occurrences (Figure 1a – averaging along the  $\zeta$ -axis, i.e. over the entire set of occurrences – ensemble, for each time instant). This type of averaging is called probabilistic, or ensemble averaging. Spatial averaging emerged more than a hundred years later (during the 1960s). It arose from the need to mathematically describe laminar flow in a two-phase (solid soil grains and water) porous medium (Figure 1b). Darcy described one-dimensional spatially heterogeneous flow using an apparent, so-called, Darcy velocity. The velocity is equal to the volume discharge divided by the cross-sectional area perpendicular to the flow. The cross-sectional area includes both the grains (solid phase) and pores between grains. The well-known Darcy’s law was formulated in 1856 based on laboratory experiments of flow through a column filled with sand. A hundred and thirty years later, Whitaker derived Darcy’s law by spatial averaging of Navier-Stokes equations [45] thus showing that Darcy’s velocity is a volume-averaged, global flow velocity and not the one at which fluid particles travel through the pores. There was no need for time averaging since only laminar flow was considered. The first idea for coupling time and spatial averaging originates from micrometeorologists who noticed notable discrepancies between measured and calculated temperature

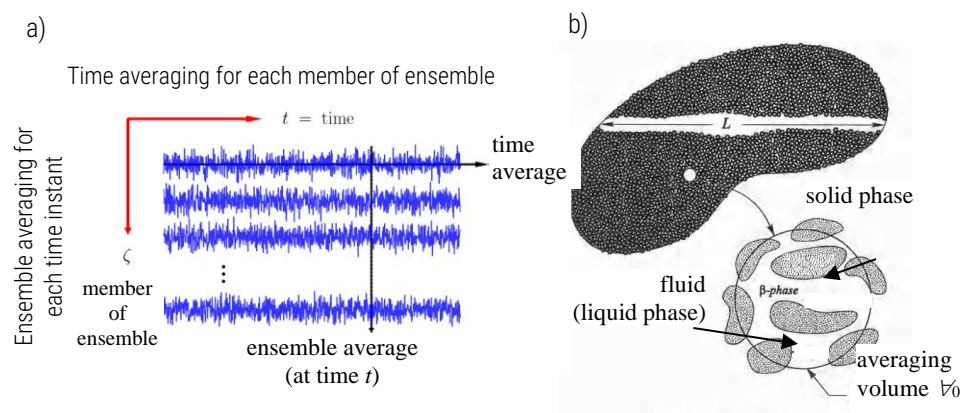


Figure 1 a) Time and ensemble averaging [2]. Time averaging is done for each member of ensemble (experiment or field measurement). Ensemble averaging is performed at a time instant for all members of ensemble. b) Two-phase porous medium with the enlarged averaging volume (adapted from [5 and 45])

and moisture fields when simulating turbulent flow (wind) over and through terrestrial vegetation by using time-averaged (Reynolds averaged) Navier-Stokes equations with a classical turbulence models closures. These include Boussinesq eddy viscosity or Prandtl mixing length turbulence models, which use velocity gradient to calculate shear stresses. Moreover, Wilson and Shaw arrived to a conclusion that time averaging is not sufficient to describe the observed processes of momentum exchange and, consequently, to reproduce correctly transport processes between vegetation and lower layers of the atmosphere [48]. They attributed these discrepancies to the spatial heterogeneity of the flow field caused by vegetation. Thus, they proposed additional, spatial averaging of the time-averaged Navier-Stokes equations (Reynolds averaged Navier-Stokes or RANS equations) over horizontal area that is sufficiently large to provide statistical averaging of all variations caused by irregular spacing between stems and large eddies through which the momentum transfer occurs [48]. Further to Wilson and Shaw, with this mathematically rigorous double averaging procedure, first in time and consequently in space, a set of momentum equations with all relevant forces for the description of flow and transport processes in a spatially heterogeneous domain are obtained. It is emphasized that the forces appear through the double averaging procedure as opposed to the RANS equations where they are introduced *ad hoc*, depending on the problem under consideration. The forces emerge as new terms in the equations like Reynolds stresses emerged through the time averaging process of Navier-Stokes equations. Wilson and Shaw suggest that the Reynolds stresses are modelled with the transport equations for Reynolds stresses and that the terms resulting from double averaging are parametrised based on laboratory experiments or field measurements. Raupach and Shaw [36], Raupach et al. [37], and Finnigan [13, 14] consequently improved the double averaging procedure/methodology for Navier-Stokes equations in micrometeorology. The most notable improvement was that of Finnigan in 1985 when he proposed spatial averaging of RANS over thin horizontal layers instead of their spatial averaging over horizontal planes.

The flow in gravel-bed rivers is highly turbulent both during low and high flows. During low flows, water flows around and between boulders and gravel making the flow field spatially heterogeneous. At high flows, roughness elements (boulders and large gravels) are submerged. However, due to their random distribution and variable height, the flow field is also spatially heterogeneous. The possibilities of applying DAM in fluvial hydraulics of gravel-bed rivers was recognised in the late 1990ies and early 2000s by a group of authors gathered around Vladimir Nikora. They formed a task group under the auspices of IAHR (International Association of Hydraulic Research) aiming at deriving equations suitable for the analysis of spatially heterogeneous,

turbulent open-channel flows. As with micrometeorologists, spatial averaging was initially performed over horizontal planes. However, very soon it was substituted with the averaging over thin layers parallel to the mean bed-line. The working group also investigated and discussed if the order of averaging (first in time and second in space, or vice versa) affected the results of double averaging. After detailed mathematical

analyses and derivations, they arrived to the conclusion that the final solution was independent of the averaging sequence on condition that the bed was fixed or that roughness elements were still or moved slowly thus not affecting the shape of the bed. In this manner, they proved the commutativity of the time and spatial averaging operators. Pokrajac et al. [34] presented this visually with the averaging matrix that will be shown in section 3 Double averaged Navier-Stokes equations.

Apart from the analysis of flow over fixed rough beds, DAM was successfully applied to flow over movable rough bed [26 and 31] and breaking waves (oscillatory flow) on the seashore where there is a permanent interaction between the waves and movable rough bed, whose roughness stems either from gravels and boulders or from bedforms on sandy beaches [15]. Additionally, the DAM becomes indispensable tool in data processing of big data collected during experiments or from direct numerical simulations, when they should be presented in such a way to provide usable information.

Aquatic and riparian vegetation, which grows in rivers and streams, or irrigation and drainage and navigable canals also make the flow field spatially heterogeneous. Inspired by Raupach and Finnigan, Poggi et al. [29 and 30] studied the flow field in a laboratory canal with submerged rigid cylinders (Figure 2) using the Laser-Doppler Anemometer (LDA) as a non-invasive measurement technique. The results revealed the effect of vegetation density on the turbulence flow structure in layers influenced by its presence. Based on these findings, Poggi et al. proposed: 1) a model of flow in the canopy sublayer – CLS, 2) parametrisation for the drag coefficient of the array of cylinders and 3) a new model for the mixing length. Tannino and Nepf [39 and 40] used the DAM to analyse lateral dispersion inside the area of randomly distributed emergent rigid cylinders and to parametrise the drag coefficient of such group of cylinders. The method was also used by other researchers from Heidi Nepf laboratory at MIT for the analysis and interpretation of the experimental data of open channel vegetated flow [21, 23, 27]. Nikora et al. [24] applied DAM to analyse measured velocity profiles in a grassy channel and proposed a new, general expression for the velocity distribution through the water depth, which takes into account all four mechanisms that affect velocity distribution. They are: 1) the effect of vegetation through which the water flows with a constant velocity thus giving a uniform velocity distribution, 2) mixing in the shear layer at the top of vegetation, which is a consequence of the inflection point in the vertical distribution of the double-averaged velocity (mixing layer analogy), 3) turbulence in the boundary layer above the vegetation where velocity follows the logarithmic law (boundary layer concept) and 4) turbulence in the free flow outside the boundary layer with vortices of different size and frequency (wake function concept).

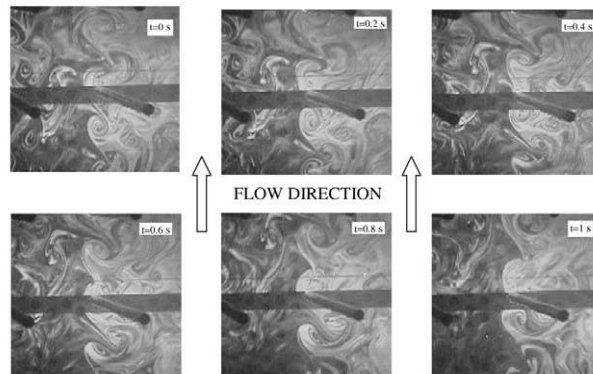


Figure 2: Development of vortices between submerged rigid cylinders [29]



Figure 3: Lonjsko polje during floods [38]. Lonjsko polje is a planned flood retention pond used as an active flood control measure. This reforested area is used to retain a part of the flood wave volume

The effect of floodplain vegetation was experimentally studied by research groups from Finland [1, 7], Germany [18] and the Netherlands [22]. Numerical studies of open channel vegetated flows are scarce and they mainly use commercial software with RANS or shallow water equations. In these equations, effects of vegetation are taken into account by adding *ad hoc* the term describing the form drag due to vegetation [3, 4, 8, 17, 35, 44]. As floodplain vegetation makes the flow field spatially heterogeneous during overbank flows, the Double Averaging Methodology makes a solid ground for floodplains reforestation planning (Figure 3) as a measure to alleviate economic and social consequences of floods. The application of the Double Averaging Methodology to modelling open channel vegetated flows was the subject of the recently finished project DoubleVeg that was financed by the Science Fund of the Republic of Serbia within the Diaspora call.

In the section 2, basic principles of DAM are presented, first. Consequently, the methodology is applied to Navier-Stokes equations to arrive to Double Averaged Navier Stokes (DANS) equations. The DANS equations are the basis for the derivation

of the mathematical model of open-channel vegetated flow. They are integrated over the flow depth in the section 3 and a new set of equations is derived. These are Depth Integrated Double Averaged Navier-Stokes (DIDANS) equations. The application of the existing finite-volume methods to solving DIDANS equations is not straightforward. The fact that a physical property of the flow domain, namely a porosity caused by the presence or absence of vegetation, may change in space, must be taken into account when discretising DIDANS equations. This issue is discussed in subsection 3.2. Finally, results of testing homogeneous DIDANS equations with spatially variable distribution of vegetation (spatially variable porosity in the flow domain) are presented to demonstrate the adequacy of the applied solution method. Additionally, some initial results of ongoing testing of non-homogeneous equations with selected, individual, source term are shown. In the end, the most important conclusions are summarised and directions for further research are highlighted.

## 2 DOUBLE AVERAGING

### 2.1 THEORETICAL BACKGROUND

Double averaged Navier-Stokes equations, double averaged continuity equation and double averaged transport equations for scalar variables such as the temperature, passive substances and suspended sediments can be derived in two ways, which differ in an averaging sequence. In one of them Navier-Stokes (NS) equations are first averaged in time and then in space (time-space averaging), while in the other one spatial averaging precedes time averaging (space-time averaging). After long discussions and detailed theoretical analyses [10 and 27], the IAHR task group for the application of DAM to modelling spatially heterogeneous, turbulent open-channel flows arrived to a conclusion that the final result is independent of the averaging sequence [27 and 34]. This will be illustrated in an example of spatially averaged Reynolds stresses [34].

While spatial-time averaging is used in groundwater hydraulics and modelling of flows in porous medium, the time-spatial averaging is intuitively close to micrometeorologists and open-channel hydraulicians, because they register time-series of kinematic and scalar variables in a finite number of points, i.e. very small finite volumes. By averaging over statistically representative intervals spatially heterogeneous fields of time-averaged velocities and scalar variables is obtained (Figure 4). Such fields are consequently averaged in space over a suitable averaging volume to capture statistically representative sample of spatially heterogeneous flow.

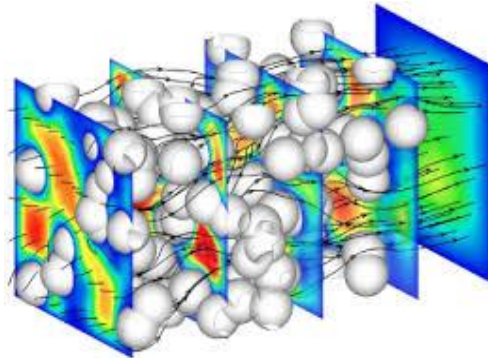


Figure 4: Flow through a porous medium: time-averaged, spatially heterogeneous flow field [9]

Results obtained in this manner do not depend on the size of the volume. In open-channel flows over rough beds, statistically representative volume is a thin layer parallel to the mean bed (Figure 5). The integration volume is around the point  $x_i$ , and integration is performed in the local coordinate system  $\xi$ . In open-channel flows, the subscript 1 in the global coordinate system refers to the axis directed in the main flow direction, which is parallel to the mean bed. This is the  $x$ -axis. The subscript 2 refers to the axis in the cross-sectional plain pointing from the left to the right bank –  $y$ -axis. Finally, subscript 3 refers to the vertical axis with the positive direction towards the free surface –  $z$ -axis. The corresponding velocity components are:  $u_1 \equiv u$ ,  $u_2 \equiv v$  and  $u_3 \equiv w$ . Through the roughness elements and closely above their crest (where the flow field is spatially heterogeneous) layers are very thin to capture the flow field in the zone of large velocity gradients. In the free flow zone, layers might be thicker as shown by Pokrajac and de Lemos [31]. However, the use of variable layer thickness introduces new terms in expressions for the averaging theorem, i.e. it requires extension of the theorem. As a result, additional terms appear in double averaged equations. The extended averaging theorem is formulated and DANS for variable averaging volumes are derived in [31]. However, the description of the double averaging procedure with volumes of variable size is beyond the scope of this paper and shall not be presented here.

Apart from its height (layer thickness), the size of the volume projection onto the mean bed parallel plain also defines the representative volume. The size of this area near the crest of roughness elements must be sufficiently large to provide statistically

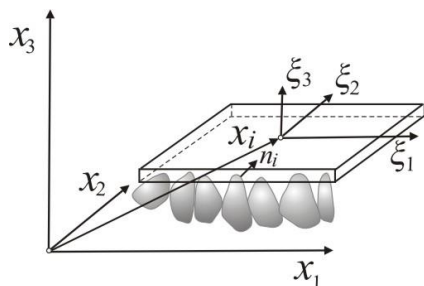


Figure 5: Representative averaging volume for spatial averaging in global  $(x_1, x_2, x_3)$  and local  $(\xi_1, \xi_2, \xi_3)$  coordinate systems. Below the crest of roughness elements it captures both fluid and solid phase (grains) [26]. Position vector of the averaging volume is denoted by  $x_i$ , and unit vector normal to the solid boundary, which is directed towards the fluid is denoted by  $n_i$

representative sample of spatially heterogeneous flow – it must capture vortices of all sizes caused by the flow detachment from the crest of roughness elements. Yet, it has to be small enough to avoid inclusion of big elements in the bottom relief such as chutes and polls in mountainous streams [28] or bars in braided rivers no matter whether it is a middle course stretch where the river sediment is coarser or the lower course where the sediment is finer.

The representative volume near the bed  $\forall 0$  captures both the fluid and the solid phase. Any quantity  $\theta$  can be averaged over the entire representative volume  $\forall 0$ . Such a quantity is denoted by  $\langle \theta_s \rangle$ . Arbitrarily, it can be averaged only in the part of the representative volume which is occupied with the fluid  $\forall f$ . In the latter case it is denoted only with the angled bracket  $\langle \theta \rangle$ . The angled bracket indicates the spatially averaged quantity. The subscript “s” is used to designate fictive volume averaged value, meaning that this is rather a pure computational category, than a physical quantity (such as Darcy velocity, for example). This is a so-called “superficial average”. Averaging over the part of the volume occupied with fluid  $\forall f$  gives the so-called “intrinsic average”. The intrinsic average  $\langle \theta \rangle$  used in open-channel hydraulics.

The spatial averaging procedure is equivalent to data filtering and can be presented using the convolution integral with the appropriate kernel function. The simplest filter is the one that uses uniform kernel function [27]:

$$\gamma(x, t) = \begin{cases} 1, & \text{in the part of the volume occupied with fluid} \\ 0, & \text{in the remaining part of the volume} \end{cases} \quad (1)$$

With this kernel function superficial and intrinsic averages are determined in the following way [27]:

$$\langle \theta \rangle_s(x_i, t) = \frac{1}{\forall_0} \int_{\forall_0} \theta(x_i + \xi_i, t) \gamma(x_i + \xi_i, t) d\forall = \frac{1}{\forall_0} \int_{\forall_f} \theta(x_i + \xi_i, t) d\forall \quad (2a)$$

$$\langle \theta \rangle(x_i, t) = \frac{1}{\forall_f} \int_{\forall_0} \theta(x_i + \xi_i, t) \gamma(x_i + \xi_i, t) d\forall = \frac{1}{\forall_f} \int_{\forall_f} \theta(x_i + \xi_i, t) d\forall \quad (2b)$$

The quantity  $\theta$  can be a scalar, a vector or a tensor. The intrinsic average for the uniform kernel function is  $\langle \gamma \rangle = 1$ . The fluid volume  $\forall_f$  inside the averaging volume  $\forall_0$  is:

$$\forall_f = \int_{\forall_0} \gamma(x_i + \xi_i, t) d\forall. \quad (3)$$

The two operators for spatial averaging are connected via parameter  $\phi$ . Nikora et al. interpret this parameter either as a function of the geometry of roughness elements or as a porosity  $\phi = \forall_f / \forall_0$  [27].

The value of a quantity  $X$  at a point can be presented as a sum of its spatially averaged value  $\langle X \rangle$  and the deflection from its spatially averaged value (spatial disturbance)  $\tilde{X}$ :  $X = \langle X \rangle + \tilde{X}$ . As in the time averaging, where the fluctuation average equals zero ( $\langle \tilde{X}' \rangle = 0$ ), the spatial average of the „spatial disturbance“ is equal zero:  $\langle \tilde{X} \rangle = 0$ .

The sparial averaging rules for the sum and the product are the same as in the time (or Reynolds) averaging:

1. Spatially averaged value of the sum equals the sum of the spatial averages:

$$\langle X + Y \rangle = \langle X \rangle + \langle Y \rangle \quad (4)$$

2. Spatially averaged value of the product of the constant and some quantity at a point equals the product of the constant and the spatially averaged value of the quantity:

$$\langle a X \rangle = a \langle X \rangle \quad (5)$$

3. Spatially averaged value of the product of the spatially averaged and instantaneous values equals the product of spatially averaged values:

$$\langle \langle X \rangle Y \rangle = \langle X \rangle \langle Y \rangle \quad (6)$$

To apply this rule it is necessary that the condition of representativeness of the averaging volume is fulfilled [27].

4. The expression for the spatially averaged value of the product is derived in a similar manner as the time-averaged value of the product. The derivation is based on the rule 3, i.e. expression (6) and the fact that the spatially averaged value of the “spatial fluctuation” is zero:

$$\langle X Y \rangle = \langle X \rangle \langle Y \rangle + \langle \tilde{X} \tilde{Y} \rangle \quad (7)$$

The presented splitting of the quantity into its averaged value and spatial fluctuation and rules 1-4 stand for both instantaneous and time-averaged quantity, and they can be even applied to temporal fluctuation.

Since the domain of averaging depends on the four dependent variables – time  $t$  and three spatial coordinates  $x_i$ , the operators of the spatial averaging and differentiation are not commutative. Thus, the rules for spatial averaging of derivatives require



introduction of theorems that establish the relationship between spatially averaged derivatives of a quantity and the derivative of that spatially averaged quantity. There are two such theorems – one for the time derivative, and the other for the spatial derivative. Both theorems were proposed by researchers dealing with multiphase flows and flow in porous medium in the late 1960ies. The theorems have been shaping since then as different solutions to different problems from these fields were sought for. The latest versions of these theorems together with their derivation can be found in [46].

The theorem on averaging the time derivative of a quantity over the entire in known as *the transport theorem* and it reads [46 and 27]:

$$\left\langle \frac{\partial \theta}{\partial t} \right\rangle_s = \frac{\partial \langle \theta \rangle_s}{\partial t} + \frac{1}{\nabla_0} \iint_{A_{s,int}} \theta v_i n_i dA \quad (8)$$

In the part of the volume occupied with fluid it transforms to:

$$\left\langle \frac{\partial \theta}{\partial t} \right\rangle = \frac{1}{\phi} \frac{\partial \phi \langle \theta \rangle}{\partial t} + \frac{1}{\nabla_f} \iint_{A_{s,int}} \theta v_i n_i dA \quad (9)$$

All quantities in these expressions except the area of the solid phase have been already described;  $A_{s,int}$  is the total area of all elements of the solid phase within the averaging volume and  $n_i$  is the unit vector of the normal to the solid boundary, which is directed towards the fluid. In the fixed-bed case, which is considered in this paper, the second term in equations (8) and (9) equals zero, because the moving velocity of the solid boundary is

zero ( $v_i = 0$ ).

The second theorem is the so-called *spatial-averaging theorem* and concerns the spatial derivative. The averaged spatial derivative over the entire volume (superficial average) is defined as [46 and 27]:

$$\left\langle \frac{\partial \theta}{\partial x_i} \right\rangle_s = \frac{\partial \langle \theta \rangle_s}{\partial x_i} - \frac{1}{\nabla_0} \iint_{A_{s,int}} \theta n_i dA \quad (10)$$

and over the volume occupied with fluid (intrinsic average) as:

$$\left\langle \frac{\partial \theta}{\partial x_i} \right\rangle = \frac{1}{\phi} \frac{\partial \phi \langle \theta \rangle}{\partial x_i} - \frac{1}{\nabla_f} \iint_{A_{s,int}} \theta n_i dA \quad (11)$$

As in the case of spatial averaging rules 1-4, the quantity  $\theta$  can be either instantaneous or time-averaged. This is important for the double averaging procedure in which time averaging precedes spatial averaging. Nikora et al. [27 and 26] suggested spatial-averaging theorems of the time-averaged variables for different cases – from flow over the fixed rough bed, to the flow over the movable rough bed either bare, only covered with sediments or covered with flexible aquatic vegetation. In this paper, only theorems for the fixed bed case are considered ( $u_i = 0$ ).

## 2.2 DOUBLE AVERAGED NAVIER-STOKES EQUATIONS

Double averaging is performed through the application of time and space averaging procedures to each equation, which is then followed by the application of the rules 1-4 for sum and product averaging and averaging theorems. It should be noted that all four operators, used in double averaging, are commutative. These are averaging operators (for time and space averaging) and both fluctuations (time and spatial fluctuations). Further to Reynolds averaging rules, the instantaneous value of  $\theta$  at an arbitrary point in space can be decomposed into its time-averaged value and its fluctuation:  $\theta = \bar{\theta} + \theta'$ . The time-averaged value  $\bar{\theta}$  can be further decomposed into its double averaged value  $\langle \bar{\theta} \rangle$  and spatial disturbance of the time-averaged value at the point from its double averaged value  $\tilde{\bar{\theta}}$ :  $\bar{\theta} = \langle \bar{\theta} \rangle + \tilde{\bar{\theta}}$ . The latter expression is obtained when the general expression for the decomposition of the quantity at a point (into its spatial average and the spatial disturbance) is applied to the time-averaged quantity  $\bar{\theta}$ . The reader is reminded that the general expression is also applicable to the instantaneous value and the fluctuation.

Upon double averaging, Navier-Stokes (NS) equations are written using the intrinsic averages of all variables. One must bear in mind that the following holds for the incompressible fluid:  $\rho = \bar{\rho} = \langle \bar{\rho} \rangle = \text{const}$ .

For the sake of easier comprehension of the double averaging process, the mass conservation and Navier-Stokes are written first:

$$\frac{\partial \rho}{\partial t} + \frac{\partial (\rho u_i)}{\partial x_i} = 0 \quad (12)$$

$$\frac{\partial u_i}{\partial t} + \frac{\partial (u_i u_j)}{\partial x_j} = g - \frac{1}{\rho} \frac{\partial p}{\partial x_i} + \frac{\partial}{\partial x_j} \left( \nu \frac{\partial u_i}{\partial x_j} \right) \quad (13)$$

### 2.2.1 Double averaged mass conservation equation

Time and space averaged equation is:

$$\left\langle \frac{\partial \rho}{\partial t} + \frac{\partial (\rho u_i)}{\partial x_i} \right\rangle = \left\langle \frac{\partial \rho}{\partial t} \right\rangle + \left\langle \frac{\partial \rho u_i}{\partial x_i} \right\rangle = 0 \quad (14)$$

Taking into account the starting assumption that the fluid is incompressible and following the rules given in (5), (6) and (9), the first term in the equation can be written as follows:

$$\left\langle \frac{\partial \rho}{\partial t} \right\rangle = \frac{1}{\phi} \frac{\partial \phi \langle \rho \rangle}{\partial t} = \frac{\rho}{\phi} \frac{\partial \phi}{\partial t} \quad (15)$$

The second term can be written following (5), (6) and (11) as:

$$\left\langle \frac{\partial \overline{\rho u_i}}{\partial x_i} \right\rangle = \frac{1}{\phi} \frac{\partial \phi \langle \overline{\rho u_i} \rangle}{\partial x_i} - \frac{1}{\nabla_f} \int \int_{A_{y, z}} \overline{\rho u_i} n_i dA \stackrel{0}{=} = \frac{1}{\phi} \frac{\partial \phi \rho \langle \overline{u_i} \rangle}{\partial x_i} = \frac{\rho}{\phi} \frac{\partial \phi \langle \overline{u_i} \rangle}{\partial x_i} \quad (16)$$

The resulting double averaged mass conservation equation finally reads:

$$\left\langle \frac{\partial \rho}{\partial t} + \frac{\partial (\rho u_i)}{\partial x_i} \right\rangle = \frac{\partial \phi}{\partial t} + \frac{\partial \phi \langle \overline{u_i} \rangle}{\partial x_i} = 0 \quad (17)$$

It can be noticed that in the double averaged mass conservation equation the fluid density  $\rho$  is supplemented with the porosity  $\phi$ . In the fixed bottom case, the porosity does not change over time. Thus, the first term on the left hand-side in (17) is zero. Additionally, when the bed material is homogeneous, porosity is constant in space and the mass conservation equation has the same form as that for the incompressible fluid, except it contains the double averaged velocity instead of the instantaneous velocity at a point.

### 2.2.2 Double averaged momentum conservation equation

Similar to the double averaging of the mass conservation equation, the double averaging procedure of all terms in Eq.(13), except the convective term with the partial derivative of the velocity product ( $\partial(u_i u_j) / \partial x_j$ ) is simple. It follows the averaging rules (4)-(7) and averaging theorems (9) and (11). Therefore, a special attention is paid to the double averaging procedure of this term.

Spatial averaging of the time-averaged velocity product  $\overline{u_i u_j}$  (the kinematic form of the flux of momentum  $\rho u_i$  in the  $j^{\text{th}}$  direction), by applying all time and space averaging rules and keeping in mind the commutativity of the four operators gives:

$$\begin{aligned} \langle \overline{u_i u_j} \rangle &= \langle \overline{u_i \bar{u}_j} + \overline{u'_i u'_j} \rangle = \langle \bar{u}_i \bar{u}_j \rangle + \langle u'_i u'_j \rangle = \langle \bar{u}_i \rangle \langle \bar{u}_j \rangle + \langle \tilde{u}_i \tilde{u}_j \rangle + \langle u'_i u'_j \rangle = \\ &= \langle \bar{u}_i \rangle \langle \bar{u}_j \rangle + \langle \tilde{u}_i \tilde{u}_j \rangle + \langle u'_i \rangle \langle u'_j \rangle + \langle \tilde{u}'_i \tilde{u}'_j \rangle \end{aligned} \quad (18)$$

The same expression is obtained when the spatially averaged product  $\langle u_i u_j \rangle$  is averaged over time:

$$\begin{aligned} \overline{\langle u_i u_j \rangle} &= \overline{\langle u_i \rangle \langle u_j \rangle} + \overline{\langle \tilde{u}_i \tilde{u}_j \rangle} = \overline{\langle u_i \rangle} \overline{\langle u_j \rangle} + \overline{\langle \tilde{u}_i \tilde{u}_j \rangle} = \langle \bar{u}_i \rangle \langle \bar{u}_j \rangle + \langle u'_i \rangle \langle u'_j \rangle + \langle \tilde{u}_i \tilde{u}_j \rangle = \\ &= \langle \bar{u}_i \rangle \langle \bar{u}_j \rangle + \langle u'_i \rangle \langle u'_j \rangle + \langle \tilde{u}_i \tilde{u}_j \rangle + \langle \tilde{u}'_i \tilde{u}'_j \rangle \end{aligned} \quad (19)$$

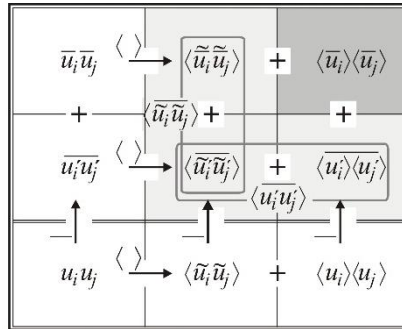


Figure 6. Double averaging matrix according to [34]. All momentum fluxes are divided by the density  $\rho$  and multiplied by  $(-1)$

This means that the order of averaging – time/space or space/time does not influence the result of double averaging. Pokrajac et al. [34] presented this visually with the matrix of spatial and temporal averaging (Figure 6). The averaging process starts in the lower right corner where an instantaneous ‘kinematic’ momentum flux  $u_i u_j$  at a point is located. Temporal averaging is performed from the bottom row upwards ( $\uparrow$ ), while the spatial averaging is performed from left to right ( $\rightarrow$ ). Thus, results of temporal averaging are presented in columns, and those of spatial averaging in rows. Irrespective of the averaging order, two additional terms in the double averaged equation are obtained. Due to commuting properties of the averaging and disturbance operators, temporal averaging ( $\uparrow$ ) produces in all columns time-averaged product of fluctuations  $\overline{u'_i u'_j}$  and the product of time averages  $\overline{u_i u_j}$ . On the other hand, spatial averaging ( $\rightarrow$ ) produces in all rows spatially averaged product of spatial disturbances  $\langle \tilde{u}_i \tilde{u}_j \rangle$  and the product of spatially averaged values  $\langle \bar{u}_i \bar{u}_j \rangle$  [34].

It can be noticed that double averaging of the ‘kinematic’ momentum flux  $u_i u_j$  four additional terms are obtained (shaded cells). One of them contains product of double averaged velocities (dark grey), while the three remaining terms (light gray), when multiplied with  $-\rho$ , are apparent stress terms. When grouped with the double averaged viscous stress  $\rho \nu \langle \partial \bar{u}_j / \partial x_i \rangle$  they give so-called “macroscopic stress”:

$$\tau_{ij}^f = \rho \left( \nu \left\langle \frac{\partial \bar{u}_j}{\partial x_i} \right\rangle - \langle \tilde{u}_i \tilde{u}_j \rangle - \overline{\langle u'_i \rangle \langle u'_j \rangle} - \langle \overline{u'_i u'_j} \rangle \right) \quad (20)$$

The apparent stress term  $-\rho \langle \tilde{u}_i \tilde{u}_j \rangle$  results from disturbances in time-averaged velocity profiles caused by the arbitrary distribution and shape of the roughness elements. Nikora et al. named this term *form-induced stress* [27]. In micrometeorology, groundwater hydraulics and hydraulics of multiphase flows this term is called *dispersive stress* [27 and 34]. When the flow field is homogeneous, this stress is zero. Spatially averaged Reynolds stress  $-\rho \langle \overline{u'_i u'_j} \rangle$  has two components: „macro“ component  $-\rho \overline{\langle u'_i \rangle \langle u'_j \rangle}$  or large-scale turbulence stress and the “micro”

component  $-\rho \left\langle \overline{\tilde{u}'_i \tilde{u}'_j} \right\rangle$ , or small-scale turbulence stress. Pokrajac et al. [34] give the

following interpretation of the two components. The micro component results from vortices smaller than the spatial averaging volume, while macro component results from the fluctuations produced by vortices larger than the spatial averaging volume. With the reduction of the averaging volume, the macroscopic component of the spatially averaged Reynolds stress prevails. On the other hand, when the averaging volume increases, small-scale turbulence stresses become dominant.

Now that the double averaging of the flux of momentum  $\rho u_i$  in the  $j^{\text{th}}$  direction is completed, double averaged momentum conservation equations divided by  $\rho$  (DANS equations) can be written:

$$\begin{aligned} \underbrace{\frac{\partial \langle \bar{u}_i \rangle}{\partial t}}_{\text{I}} + \underbrace{\frac{1}{\phi} \frac{\partial \phi \langle \bar{u}_i \rangle \langle \bar{u}_j \rangle}{\partial x_j}}_{\text{II}} = \underbrace{g_i}_{\text{III}} - \underbrace{\frac{1}{\rho \phi} \frac{\partial \phi \langle \bar{p} \rangle}{\partial x_i}}_{\text{IV}} + \underbrace{\frac{1}{\rho \phi} \frac{\partial \phi \tau_{ij}^f}{\partial x_j}}_{\text{V}} \\ + \underbrace{\frac{1}{\rho} \frac{1}{\phi} \frac{1}{\nabla_f} \iint_{A_{s.int.}} \bar{p} n_i dA}_{\text{VI}} - \underbrace{\frac{1}{\phi} \frac{1}{\nabla_f} \iint_{A_{s.int.}} \nu \frac{\partial \bar{u}_i}{\partial x_j} n_i dA}_{\text{VII}} \end{aligned} \quad (21)$$

Similarly to the time averaging of the Navier-Stokes equations, which produced Reynolds stresses (see [16]), introduction of additional averaging step to the time-averaged Navier-Stokes equations or Reynolds averaged Navier-Stokes equations (spatial averaging of time-averaged values and fluctuations) produces new terms in the averaged equations. In addition to the already presented apparent stresses (three new terms) that enter with the spatially averaged viscous stress into the macroscopic stress (20) appearing in the term V, the new term is the friction force between the fluid and the roughness elements, per unit volume. This force is obtained by double averaging of the derivative of the viscous stress (the last term in Eq.(13)). The friction force is the term VII. The application of the double averaging theorem (11) to the term that describes pressure force per unit mass in the NS equations, one more additional term appears in DANS equations – the term VI in (21). This is the drag force per unit fluid volume of the roughness elements, which is usually entered *ad hoc* into Reynolds equations.

The remaining terms in the double averaged momentum equation (21) are: double averaged local acceleration (the term I), double averaged derivative of the flux of momentum  $\rho u_i$  per unit mass in the  $j^{\text{th}}$  direction (the term II), acceleration due to gravity (the term III) and the derivative of the double averaged pressure (the term IV). In the momentum equation terms III and IV are the so-called “source terms” (forces which add momentum to the fluid). The term V is the transport term, which describes how the real and apparent forces are transported through the fluid layers and between different flow zones. Terms VI and VII are the so-called “sink terms” which extract momentum from the fluid flow.

### 3 DERIVATION OF DIDANS EQUATIONS FOR OPEN-CHANNEL VEGETATED FLOWS AND THEIR NUMERICAL SOLUTION

Like Navier-Stokes and Reynolds Averaged Navier-Stokes equations, Double Averaged Navier-Stokes equations mathematically describe three-dimensional (3D) flow. However, models of 3D flow are still impractical for engineering applications such as planning of floodplains reforestation, which is nowadays recognised as a measure to alleviate economic and social consequences of floods. Two-dimensional (2D) models are less consuming and allow estimation of different planting strategies on the flood extent, reduction of the peak discharge and a delay in reaching it downstream of the applied measure(s), as well as the estimation of an increase in flood levels upstream of the forested area. One-dimensional (1D) models are the most robust in that respect, and, from the model developer's point of view, they are the basis on which the development of higher dimension numerical models rest.

This section will present the derivation of the Depth Integrated Double Averaged Navier-Stokes (DIDANS) equations (2D and 1D) for open-channel vegetated flows with arbitrary distribution of vegetation patches first. Due to the novelty of the mathematical model, the existing numerical methods are not directly applicable to solving these equations. Until now, a solution has only been found for homogeneous one-dimensional DIDANS equations and it will be presented after the model derivation procedure, along with the results of model testing against the analytical solution for the simplified geometry.

#### 3.1 DIDANS EQUATIONS

These equations are a special case of the General Shallow Water Equations [32] recently derived by the partner in the DoubleVeg project from diaspora. They are derived by integrating DANS equations over the depth under the following assumptions: the free-surface is flat and parallel to the mean bed, the flow is 2D in vertical  $xOz$  plain (all derivatives in the direction perpendicular to the main flow direction ( $x$ -direction) are zero, i.e.  $\partial/\partial y = 0$ ), and vegetation is rigid and can be approximated by straight cylinders of constant diameter, thus ensuring constant porosity throughout the flow depth (Figure 7). The averaging volume is a thin layer parallel to the sloping bottom whose base is large enough to provide statistically representative sample of vegetated flow.

A depth-integrated value of an arbitrary variable  $\theta$  is [11]:

$$\langle \theta \rangle_d = \frac{1}{h} \int_{\bar{z}_b}^{\bar{z}_s} \theta dz \quad (22)$$

where  $h$  is the flow depth in the  $z$ -direction which is perpendicular to the bottom (the distance between the water surface  $\bar{z}_s$  and the mean bed  $\bar{z}_b$ , Figure 7). The variable  $\theta$  can be expressed as the sum of the depth-integrated value  $\langle \theta \rangle_d$  and its departure from this value at the point  $\theta^d$ :  $\theta = \langle \theta \rangle_d + \theta^d$ . The depth-integrated value of the

departure is zero ( $\langle \tilde{\theta}^d \rangle_d = 0$ ). When (22) is applied to the double averaged velocity  $\langle \bar{u} \rangle$  in the main flow direction  $x$ , a triple averaged velocity  $\langle \langle \bar{u} \rangle \rangle_d = U$  is obtained, and the double averaged velocity can be presented as [11]:

$$\langle \bar{u}_i \rangle = \langle \langle \bar{u}_i \rangle \rangle_d + \langle \bar{u}_i \rangle^d = U + \langle \bar{u}_i \rangle^d \quad (23)$$

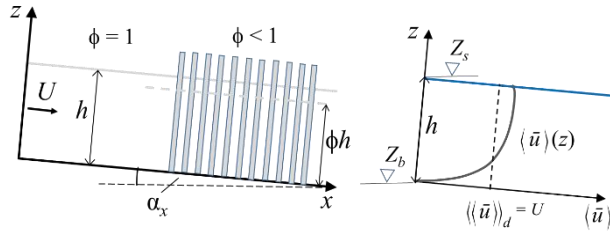


Figure 7. a) Coordinate system in which thin layers for spatial averaging are defined. Thin layers are parallel to the bottom, which is inclined at an angle  $\alpha_x$  to the horizontal. The  $x$ -axis is along the bottom. The  $z$ -axis and rigid vegetation are perpendicular to the bottom. b) Double averaging of Navier-Stokes equations results in double averaged streamwise velocity profile along the flow depth. Integration of the profile throughout the flow depth gives triple averaged velocity  $U$  – see expression (23) [11]

### 3.1.1 Depth integration of the double averaged mass conservation equation

Double averaged mass conservation equation (17) is integrated over the depth following (22), under the assumption that the porosity does not change within the time averaging window. The remaining term is the one with the partial derivative  $\partial/\partial x$ . It is integrated using Leibnitz integral rule:

$$\begin{aligned} \frac{1}{h} \int_{\bar{z}_b}^{\bar{z}_s} \frac{\partial \phi \langle \bar{u}_i \rangle}{\partial x_i} dz &= \frac{1}{h} \left[ \int_{\bar{z}_b}^{\bar{z}_s} \frac{\partial \phi \langle \bar{u} \rangle}{\partial x} dz + \int_{\bar{z}_b}^{\bar{z}_s} \frac{\partial \phi \langle \bar{v} \rangle}{\partial y} dz + \int_{\bar{z}_b}^{\bar{z}_s} \frac{\partial \phi \langle \bar{w} \rangle}{\partial z} dz \right] = \\ &= \frac{1}{h} \left[ \frac{\partial}{\partial x} \int_{\bar{z}_b}^{\bar{z}_s} \phi \langle \bar{u} \rangle dz - \phi_s \langle \bar{u}_s \rangle \frac{\partial \bar{z}_s}{\partial x} + \phi_b \langle \bar{u}_b \rangle \frac{\partial \bar{z}_b}{\partial x} + \right. \\ &+ \frac{\partial}{\partial y} \int_{\bar{z}_b}^{\bar{z}_s} \phi \langle \bar{v} \rangle dz - \phi_s \langle \bar{v}_s \rangle \frac{\partial \bar{z}_s}{\partial y} + \phi_b \langle \bar{v}_b \rangle \frac{\partial \bar{z}_b}{\partial y} + \\ &\left. + \phi_s \langle \bar{w}_s \rangle - \phi_b \langle \bar{w}_b \rangle \right] = 0 \end{aligned} \quad (24)$$

In the previous expression, subscript “s” refers to the values at the surface and subscript “b” to the values at the bottom. Since the velocity at the bottom is zero, all terms with bottom velocities cancel. From the assumption that the free surface is flat

and parallel to the bottom it follows that  $\partial z_s / \partial x = 0$  in the considered coordinate system. Additionally,  $\partial z_s / \partial y = 0$  due to the assumption that all derivatives in the direction perpendicular to the streamwise direction are zero. Vertical velocity at the free surface is resolved from the kinematic condition at the free surface, which reads:

$$\langle \bar{w}_s \rangle = \frac{D \bar{z}_s}{Dt} = \frac{\partial \bar{z}_s}{\partial t} + \langle \bar{u}_s \rangle \frac{\partial \bar{z}_s}{\partial x} + \langle \bar{v}_s \rangle \frac{\partial \bar{z}_s}{\partial y} \quad (25)$$

The final form of the 2D depth integrated double averaged mass conservation equation after substitution of (25) into (24), rearrangement of variables and introduction of shortened notation in (23) is:

$$\phi \frac{\partial h}{\partial t} + \frac{\partial \phi h U}{\partial x} + \frac{\partial \phi h V}{\partial y} = 0 \quad (26)$$

### 3.1.2 Depth integration of the double averaged momentum equations

Depth integration is performed following the same principles and procedures that were used in the previous subsection, this time, on Eq.(21) previously multiplied by  $\phi$ :

$$\begin{aligned} \underbrace{\frac{\partial \phi \langle \bar{u}_j \rangle}{\partial t}}_I + \underbrace{\frac{\partial \phi \langle \bar{u}_i \rangle \langle \bar{u}_j \rangle}{\partial x_i}}_{II} &= \underbrace{\phi g_j}_{III} - \underbrace{\frac{1}{\rho} \frac{\partial \phi \langle \bar{p} \rangle}{\partial x_j}}_{IV} + \\ &+ \underbrace{\frac{\partial}{\partial x_i} \left[ \nu \phi \left\langle \frac{\partial \bar{u}_j}{\partial x_i} \right\rangle \right]}_{V} - \underbrace{\frac{\partial \phi \langle \bar{u}'_i \bar{u}'_j \rangle}{\partial x_i}}_{VI} - \underbrace{\frac{\partial \phi \langle \tilde{u}_i \tilde{u}_j \rangle}{\partial x_i}}_{VII} - \\ &- \underbrace{\frac{1}{\rho} f_j}_{VIII} \end{aligned} \quad (27)$$

It is necessary to define the depth integrated value of the product of two double averaged velocities before integration of each term in Eq.(27):

$$\langle \langle \bar{u}_i \rangle \langle \bar{u}_j \rangle \rangle_d = \langle \langle \bar{u}_i \rangle \rangle_d \langle \langle \bar{u}_j \rangle \rangle_d + \left\langle \langle \bar{u}_i \rangle^d \langle \bar{u}_j \rangle^d \right\rangle_d \quad (28)$$

Depth integrated terms on the left hand side of Eq. (27) are:

I- *local acceleration*

$$\frac{1}{h} \int_{\bar{z}_b}^{\bar{z}_s} \frac{\partial \phi \langle \bar{u}_j \rangle}{\partial t} dz = \frac{1}{h} \left\{ \frac{\partial h \langle \phi \langle \bar{u}_j \rangle \rangle_d}{\partial t} - \phi_s \langle \bar{u}_{j_s} \rangle \frac{\partial \bar{z}_s}{\partial t} \right\} \quad (29)$$



### II- convective acceleration

$$\frac{1}{h} \int_{\bar{z}_b}^{\bar{z}_s} \frac{\partial \phi \langle \bar{u}_i \rangle \langle \bar{u}_j \rangle}{\partial x_i} dz = \frac{1}{h} \left[ \phi_s \langle \bar{u}_{j_s} \rangle \frac{\partial \bar{z}_s}{\partial t} + \right. \\ \left. + \frac{\partial h \phi \langle \langle \bar{u} \rangle \rangle_d \langle \langle \bar{u}_j \rangle \rangle_d}{\partial x} + \frac{\partial h \langle \phi \langle \bar{u} \rangle^d \langle \bar{u}_j \rangle^d \rangle_d}{\partial x} + \right. \\ \left. + \frac{\partial h \phi \langle \langle \bar{v} \rangle \rangle_d \langle \langle \bar{u}_j \rangle \rangle_d}{\partial y} + \frac{\partial h \langle \phi \langle \bar{v} \rangle^d \langle \bar{u}_j \rangle^d \rangle_d}{\partial y} \right] \quad (30)$$

Terms on the right hand side of the Eq.(27) are forces per unit mass and they are integrated one by one.

### III- gravity acceleration

$$\frac{1}{h} \int_{\bar{z}_b}^{\bar{z}_s} \phi g dz = \frac{1}{h} \phi g h \sin \alpha_j \quad (31)$$

### IV- pressure

In the accepted coordinate system, pressure is zero.

### V- viscous stresses

$$\frac{1}{\rho h} \int_{\bar{z}_b}^{\bar{z}_s} \frac{\partial}{\partial x_i} \left[ \mu \phi \left\langle \frac{\partial \bar{u}_j}{\partial x_i} \right\rangle \right] dz = \frac{1}{\rho h} \left\{ \frac{\partial h \langle \phi \langle \tau_{jx} \rangle \rangle_d}{\partial x} + \frac{\partial h \langle \phi \langle \tau_{jy} \rangle \rangle_d}{\partial y} + \right. \\ \left. + \phi_b \left[ -\langle \tau_{jx,b} \rangle S_{0_x} - \langle \tau_{jy,b} \rangle S_{0_y} - \langle \tau_{jz,b} \rangle \right] \right\} \quad (32)$$

where  $\langle \tau_{jx,b} \rangle = \mu \phi_b \left\langle \frac{\partial \bar{u}_j}{\partial x} \right\rangle_b$  is the viscous bed shear stress in x-direction; porosity

at the bottom  $\phi_b = \phi$  according to the assumption 2,  $S_{0_x} = \partial \bar{z}_b / \partial x$  is the bottom slope in the streamwise, x-direction. The abbreviations for the remaining two terms are made analogous to the previous ones.

### VI- Reynolds stress components

$$\frac{1}{h} \int_{\bar{z}_b}^{\bar{z}_s} \frac{\partial \phi \langle u'_i u'_j \rangle}{\partial x_i} dz = \frac{1}{\rho h} \left\{ - \frac{\partial h \langle \phi \langle \tau'_{jx} \rangle \rangle_d}{\partial x} - \frac{\partial h \langle \phi \langle \tau'_{jy} \rangle \rangle_d}{\partial y} + \right. \\ \left. + \phi_b \left[ \langle \tau'_{jx,b} \rangle S_{0_x} + \langle \tau'_{jy,b} \rangle S_{0_y} + \langle \tau'_{jz,b} \rangle \right] \right\} \quad (33)$$

where  $\langle \tau'_{jx,b} \rangle = -\rho \langle \overline{u'u'_j} \big|_b \rangle$  is the Reynolds stress at the bed in the  $x$ -direction;

$S_{0_x} = \partial \bar{z}_b / \partial x$  is the bottom slope in the streamwise,  $x$ -direction. The symbols for the remaining two terms are made analogous to the previous ones.

*VII- components of stress induced by non-homogeneous flow field resulting from the presence of obstacles (rigid vegetation)*

$$\frac{1}{h} \int_{\bar{z}_b}^{\bar{z}_s} \frac{\partial \phi \langle \tilde{u}_i \tilde{u}_j \rangle}{\partial x_i} dz = \frac{1}{\rho h} \left\{ - \frac{\partial h \langle \phi \langle \tau_{jx}^p \rangle \rangle_d}{\partial x} - \frac{\partial h \langle \phi \langle \tau_{jy}^p \rangle \rangle_d}{\partial y} - \right. \\ \left. - \phi_s \left[ \langle \tau_{jx,s}^p \rangle S_{\Pi_x} + \langle \tau_{jy,s}^p \rangle S_{\Pi_y} + \langle \tau_{jz,s}^p \rangle \right] + \right. \\ \left. + \phi_b \left[ \langle \tau_{jx,b}^p \rangle S_{0_x} + \langle \tau_{jy,b}^p \rangle S_{0_y} + \langle \tau_{jz,b}^p \rangle \right] \right\} \quad (34)$$

In the previous expression  $\langle \tau_{jx,s}^p \rangle = \langle \tilde{u} \tilde{u}_j \big|_s \rangle$ ,  $\langle \tau_{jx,b}^p \rangle = \langle \tilde{u} \tilde{u}_j \big|_b \rangle$  and  $S_{\Pi_x} = \partial \bar{z}_s / \partial x$ .

Other terms have analogous meaning.

*VIII- form drag*

$$\frac{1}{\rho h} \int_{\bar{z}_b}^{\bar{z}_s} f_j dz = \frac{1}{\rho} \langle f_j \rangle_d \quad (35)$$

Finally, after grouping components comprising macroscopic and microscopic stress components, the depth integrated DANS equations (DIDANS), or “shallow water” DANS equations can be written in the compact form:

$$\frac{\partial h \langle \phi \langle \bar{u}_j \rangle \rangle_d}{\partial t} + \frac{\partial h \phi \langle \langle \bar{u}_i \rangle \rangle_d \langle \langle \bar{u}_j \rangle \rangle_d}{\partial x_i} = - \phi g h \sin \alpha_j + \\ + \frac{1}{\rho} \frac{\partial}{\partial x_i} \left\{ h \left[ \langle \phi \langle \tau_{jx} \rangle \rangle_d + \langle \phi \langle \tau'_{jx} \rangle \rangle_d + \langle \phi \langle \tau_{jx}^p \rangle \rangle_d - \right. \right. \\ \left. \left. - \left\langle \phi \rho \langle \bar{u} \rangle^d \langle \bar{u}_j \rangle^d \right\rangle_d \right] \right\} - \\ - \frac{\phi_b}{\rho} \left[ \langle \tau_{ji,b} \rangle S_{0_i} + \langle \tau_{jz,b} \rangle \right] - \\ - \frac{1}{\rho} \langle f_j \rangle_d \quad , \quad i, j = 1, 2 \quad (36)$$

### 3.1.3 1D DIDANS equations

The standard approach in applying a new mathematical model to the analysis of a problem for which it is developed, assumes searching for an appropriate numerical model and solving possible numerical challenges in 1D case. Thus, a solution to the 1D DIDANS equations is presented in the following subsection. The one-dimensional version of Eqs. (26) and (36) is written using the shortened notation for triple averaged velocity  $\langle\langle\bar{u}\rangle\rangle_d = U$  and for the depth that the water would have had if the vegetation had been removed from the space it occupies  $\phi h = H$ :

- *DIDA mass conservation equation*

$$\frac{\partial H}{\partial t} + \frac{\partial UH}{\partial x} = 0 \quad (37)$$

- *DIDANS or DIDA momentum conservation equation*

$$\frac{\partial UH}{\partial t} + \frac{\partial UUH}{\partial x} = -\frac{1}{2}g \frac{\partial(H^2/\phi)}{\partial x} + gHS_{0_x} - \frac{1}{\rho} D_r \quad (38)$$

The depth integrated double averaged momentum equation, which contains new terms related to the pressure force, viscose, Reynolds and stresses due to vegetation presence is simplified. It is assumed that all depth averaged components of macroscopic and microscopic Reynolds stresses as well as those caused by the vegetation might be neglected when compared to the gravity acceleration and pressure force per unit mass (i.e. the first two terms on the right hand side of Eq. (36)) and the force per unit mass acting on the water per unit area of vegetation – internal drag force  $D_r$ , the third term on the right hand side. They can be written in the vector form:

$$\frac{\partial \mathbf{Q}}{\partial t} + \frac{\partial \mathbf{F}}{\partial x} = \mathbf{S}, \quad (39)$$

$$\mathbf{Q} = \begin{bmatrix} H \\ UH \end{bmatrix}, \quad \mathbf{F} = \begin{bmatrix} UH \\ U^2H + \frac{1}{2}g \frac{H^2}{\phi} \end{bmatrix}, \quad \mathbf{S} = \begin{bmatrix} 0 \\ gHS_{0_x} - \frac{1}{\rho} D_r \end{bmatrix}$$

where  $\mathbf{Q}$  is the vector of dependent variables,  $\mathbf{F}$  is the flux and  $\mathbf{S}$  is the source vector. The system of equations (39) together with the initial condition:

$$\mathbf{Q}(x, 0) = \mathbf{Q}^{(0)}(x) \quad (40)$$

and boundary conditions (Figure 8):

$$\begin{aligned} (Uh)(0,t) = (Uh)_0(t) \quad \text{and} \quad h(L,t) = h_{N_x}(t) \quad \text{for} \quad Fr < 1 \\ (Uh)(0,t) = (Uh)_0(t) \quad \text{and} \quad h(0,t) = h_0(t) \quad \text{for} \quad Fr > 1 \end{aligned} \quad (41)$$

defines initial boundary value problem.

### 3.2 NUMERICAL MODELLING

#### 3.2.1 Finite-volume method and the Riemann problem

The usual procedure to determine the suitability of the chosen numerical method for solving the considered system of equations is to apply the method to the homogeneous system of equations. Thus, the system (39) with  $\mathbf{S} = 0$  is analysed. This a system of hyperbolic-type equations. Finite-volume methods are nowadays the standard procedure for solving such systems in computational hydraulics, because they provide mass conservation within the control volume.

The computational domain of length  $L_x$  is divided into  $N_x$  control volumes (cells). Boundaries of the  $i^{\text{th}}$  cell are  $i-1/2$  and  $i+1/2$ . Fluxes between this cell and its neighbouring cells  $i-1$  and  $i+1$  are defined on these boundaries (Figure 8b). In uniform grids all cells have the same size  $\Delta x = x_{i+1/2} - x_{i-1/2} = \text{const} = L_x / N_x$ . Godunov proposed for such grids the scheme with the first order accuracy in 1950ies [42]:

$$\mathbf{Q}_i^{n+1} = \mathbf{Q}_i^n + \frac{\Delta t}{\Delta x} [\mathbf{F}_{i-1/2} - \mathbf{F}_{i+1/2}] \quad (42)$$

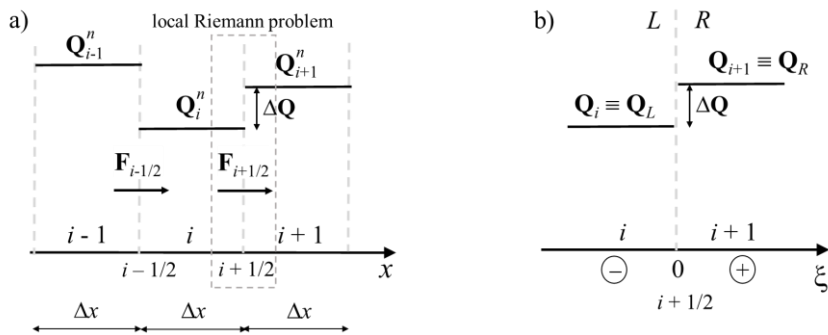


Figure 8. a) Control volumes/cells; spatially averaged values  $\mathbf{Q}$  in cells; intercell fluxes  $\mathbf{F}_{i-1/2}$  and  $\mathbf{F}_{i+1/2}$ ; dependent variables  $\mathbf{Q}$  have piecewise constant distribution in the main flow direction  $x$ . Close to the cell edge, for instance, edge  $i+1/2$ , (rectangle marked with light grey dashed line) solution to the b) local Riemann problem is sought. b) Local Riemann problem –the origin of the local coordinate system is at the common edge of the neighbouring cells. The closest point to the left is denoted by  $L$ , and that to the right by  $R$ .

where

$$\mathbf{Q}_i^n = \frac{1}{\Delta x} \int_{x_{i-1/2}}^{x_{i+1/2}} \mathbf{Q}(x, t^n) dx \quad (43)$$

is the average / spatially averaged value of  $\mathbf{Q}$  for the cell  $i$  at time  $t = t^n = n\Delta t$ , and  $\mathbf{F}_{i-1/2}$  and  $\mathbf{F}_{i+1/2}$  are intercell fluxes through the boundaries (edges) of the control volume (Figure 8a) that are used to approximate real fluxes  $\mathbf{F}(\mathbf{Q})$  in (39). These fluxes are the function of dependent variables from the opposite sides of the boundary (Figure 8a,b):

$$\mathbf{F}_{i+1/2} = \mathbf{F}_{i+1/2} (\mathbf{Q}_L, \mathbf{Q}_R) \quad (44)$$

Spatially averaged value  $\mathbf{Q}_i$  in Eq. (43) is attributed to the midpoint of the cell  $i$ . Since the spatially averaged values have piecewise constant distribution in the  $x$ -direction (Figure 8a), there is a jump in the value of each dependent variable at each cell edge. For the cell  $i$ , these jumps are  $\Delta\mathbf{Q}_{i-1/2}$  and  $\Delta\mathbf{Q}_{i+1/2}$ . This means that there is one local Riemann problem on each cell edge (Figure 8b):

$$\frac{\partial \mathbf{Q}}{\partial t} + \frac{\partial \mathbf{F}(\mathbf{Q})}{\partial x} = 0, \tag{45}$$

$$\mathbf{Q}(\xi, 0) = \begin{cases} \mathbf{Q}_L, & \text{if } \xi < 0 \\ \mathbf{Q}_R, & \text{if } \xi > 0 \end{cases}$$

that should be solved using an appropriate numerical method for the calculation of the intercell flux. In (45)  $\xi$  is a local coordinate whose origin is at the cell edge at which the local Riemann problem is solved (Figure 8b).

### 3.2.2 Solution to the Riemann problem

#### a) Nonlinear system of conservation laws with constant coefficients

Solution to the Riemann problem for the system of two partial differential equations with constant coefficients:

$$\frac{\partial \mathbf{Q}}{\partial t} + \mathbf{A} \frac{\partial \mathbf{Q}}{\partial x} = 0 \tag{46}$$

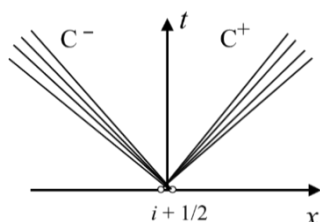


Figure 9. One of the four possible combinations of waves whose incidence is at the cell edges in the Riemann problem – two rarefaction waves; rarefaction waves are characteristic for the fan-like structure – all characteristics of one family emanate from the same point close to the cell edge. Shock waves are characteristic for the crossing of characteristics.

can be presented with four combinations of waves (characteristics) along which the information (disturbance) travels in the  $x$ - $t$  plane. The origin of these characteristics is at points immediately to the left and right of the cell edge. There are two types of waves – shock waves and rarefaction waves. Figure 9 shows one possible combination – the combination of the two rarefaction waves. Waves in each family (families 1 and 2) propagate at speeds  $\lambda_i$ ,  $i = 1, 2$ . Propagation speed of the first family (to the left) is smaller than that of the second family (to the right), i.e.  $\lambda_1 < \lambda_2$ . Wave propagation speeds show the inclination of the characteristics in the  $xOt$  plane. Mathematically, they are eigenvalues of the matrix  $\mathbf{A}$  in Eq. (46).

Each jump between the states to the left  $\mathbf{Q}_L$  and to the right of the cell edge  $\mathbf{Q}_R$  continues to propagate as a single shock wave if and only if it is a linear combination of the eigenvalues of the  $\mathbf{A}$  matrix [19]:

$$\mathbf{Q}_R - \mathbf{Q}_L = \sum_{i=1}^2 \alpha_i \mathbf{r}_i \quad (47)$$

Such a decomposition of waves is performed using the right eigenvectors of  $\mathbf{A}$ :

$$\mathbf{r}_1 = \begin{bmatrix} 1 \\ \lambda_1 \end{bmatrix}, \quad \mathbf{r}_2 = \begin{bmatrix} 1 \\ \lambda_2 \end{bmatrix} \quad (48)$$

Coefficients  $\alpha_i$  are the so-called strengths of eigenvectors.

b) *Nonlinear system of conservation laws with variable coefficients*

However, the system (45) is a system of nonlinear equations with variable coefficients. In this case, members of matrix  $\mathbf{A}$  are no longer numbers – matrix  $\mathbf{A}$  is no longer constant. It is rather a Jacobian matrix of fluxes:

$$\frac{\partial \mathbf{Q}}{\partial t} + \frac{\partial \mathbf{F}}{\partial \mathbf{Q}} \frac{\partial \mathbf{Q}}{\partial x} = 0, \quad \text{where} \quad \frac{\partial \mathbf{F}}{\partial \mathbf{Q}} = \mathbf{A}(\mathbf{Q}) \quad (49)$$

Roe proposed an efficient solution to the nonlinear system of equations with variable coefficients [19 and 42]. His idea is based on the local linearization of the system (45), i.e. on the substitution of the Jacobian matrix  $\mathbf{A}(\mathbf{Q})$  with the constant Jacobian matrix:

$$\tilde{\mathbf{A}} = \tilde{\mathbf{A}}(\mathbf{Q}_L, \mathbf{Q}_R) \quad (50)$$

which is a function of the left and right states  $\mathbf{Q}_L$  and  $\mathbf{Q}_R$  (Figure 8b). This matrix is called Roe's Jacobian matrix. In Roe's method, the system (45) is linearized at each cell edge. In this manner, the original Riemann problem is substituted with the *approximate* Riemann problem:

$$\frac{\partial \mathbf{Q}}{\partial t} + \tilde{\mathbf{A}} \frac{\partial \mathbf{Q}}{\partial x} = 0, \quad (51)$$

$$\mathbf{Q}(\xi, 0) = \begin{cases} \mathbf{Q}_L, & \text{if } \xi < 0 \\ \mathbf{Q}_R, & \text{if } \xi > 0 \end{cases}$$

which is then solved *exactly*.

Roe's Jacobian matrix must satisfy the following conditions so that the linearized system (51) keeps the hyperbolic type:

1a) eigenvalues of the matrix  $\tilde{\mathbf{A}}$  should be real and distinct:

$$\tilde{\lambda}_1 \leq \tilde{\lambda}_2 \quad (52)$$

1b) the matrix  $\tilde{\mathbf{A}}$  should have a complete set of linearly independent right eigenvectors:

$$\mathbf{r}_1 = \begin{bmatrix} 1 \\ \lambda_1 \end{bmatrix}, \quad \mathbf{r}_2 = \begin{bmatrix} 1 \\ \lambda_2 \end{bmatrix} \quad (53)$$

2- the matrix  $\tilde{\mathbf{A}}$  should be consistent with the original Jacobian matrix from (49):

$$\tilde{\mathbf{A}}(\mathbf{Q}, \mathbf{Q}) = \mathbf{A}(\mathbf{Q}) \quad (54)$$

3- Rankine-Hugoniot jump condition:

$$\mathbf{F}(\mathbf{Q}_R) - \mathbf{F}(\mathbf{Q}_L) = \tilde{\mathbf{A}}(\mathbf{Q}_R + \mathbf{Q}_L) \quad \text{or} \quad \Delta \mathbf{F} = \tilde{\mathbf{A}} \Delta \mathbf{Q} \quad (55)$$

Eigenvalues are calculated using Roe's averaged values for the primitive variables (depth and triple averaged velocities). For the sake of brevity, the following eigenvalue and eigenvector matrices are used:

$$\tilde{\mathbf{\Lambda}} = \begin{bmatrix} \tilde{\lambda}_1 & 0 \\ 0 & \tilde{\lambda}_2 \end{bmatrix} \quad \text{and} \quad \tilde{\mathbf{R}} = [\tilde{\mathbf{r}}_2 \quad \tilde{\mathbf{r}}_1] = \begin{bmatrix} 1 & 1 \\ \tilde{\lambda}_2 & \tilde{\lambda}_1 \end{bmatrix} \quad (56)$$

along with the inverse matrix  $\mathbf{R}^{-1}$ . Roe's matrix can now be written as:

$$\tilde{\mathbf{A}} = \tilde{\mathbf{R}} \tilde{\mathbf{\Lambda}} \tilde{\mathbf{R}}^{-1} \quad (57)$$

The expression for the jump in the intercell flux at the edge  $i+1/2$  then reads:

$$\Delta \mathbf{F}_{i+1/2} = (\tilde{\mathbf{A}} \Delta \mathbf{Q})_{i+1/2} = (\tilde{\mathbf{R}} \tilde{\mathbf{\Lambda}} \tilde{\mathbf{R}}^{-1} \Delta \mathbf{Q})_{i+1/2} \quad (58)$$

Consequently, Roe's numerical intercell flux at the edge between cells  $i$  and  $i+1$  for the system of homogeneous equations is [18]:

$$\mathbf{F}_{i+1/2} = \frac{1}{2} (\mathbf{F}_R + \mathbf{F}_L) - \frac{1}{2} (\tilde{\mathbf{R}} \tilde{\mathbf{\Lambda}} \tilde{\mathbf{R}}^{-1} \Delta \mathbf{Q})_{i+1/2} \quad (59)$$

The expression for the intercell flux at the edge  $i - 1/2$  is analogue to the previous one. Flux  $\mathbf{F}_R$  is calculated using the values of the vector of 1dependent variables from the right hand side  $\mathbf{F}_R = \mathbf{F}(\mathbf{Q}_R)$ , and flux  $\mathbf{F}_L$  using the values from the left hand side. These fluxes are then entered into (42) to find the solution in cell  $i$  at time  $t^{n+1}$ . The first term on the right hand side of (59) is called the central term, while the second one is called the dissipative term [22].

### 3.2.3 Adaptation of Roe's method to the DIDANS equations

The wave propagation speed in the vegetated flow is the same as in the free flow with the flow depth  $h$ :

$$c = \sqrt{\frac{gH}{\phi}} = \sqrt{gh} \quad (60)$$

Roe's-average wave propagation speed at the interface between two cells is:

$$\tilde{c} = \sqrt{0.5(c_L^2 + c_R^2)}, \quad c_L = \sqrt{\frac{gH_L}{\phi_L}}, \quad c_R = \sqrt{\frac{gH_R}{\phi_R}} \quad (61)$$

and Roe's-average depth and velocity are:

$$\tilde{h} = \sqrt{h_L h_R} \quad (62a)$$

$$\tilde{U} = \frac{U_L \sqrt{H_L} + U_R \sqrt{H_R}}{\sqrt{H_L} + \sqrt{H_R}} \quad (62b)$$

The expression for Roe's-average of triple averaged velocity  $U$  differs from that for the free flow (without vegetation). Instead of primitive variables – flow depths  $h_R$  and  $h_L$  in the free flow, dependent variables for the vegetated flow - depths  $H_R$  and  $H_L$  in DIDANS equations are used. Wave propagation speeds along the two characteristics (positive and negative) are:

$$\tilde{\lambda}_1 = \tilde{U} - \tilde{c} \quad \text{and} \quad \tilde{\lambda}_2 = \tilde{U} + \tilde{c} \quad (63)$$

and right eigenvectors:

$$\tilde{\mathbf{r}}_1 = \begin{bmatrix} 1 \\ \tilde{\lambda}_1 \end{bmatrix}, \quad \tilde{\mathbf{r}}_2 = \begin{bmatrix} 1 \\ \tilde{\lambda}_2 \end{bmatrix} \quad (64)$$

Jump at the cell interface for the dependent variables is:

$$\Delta H = H_R - H_L \quad (65a)$$

$$\Delta UH = (UH)_R - (UH)_L \quad (65b)$$

or

$$\Delta \mathbf{Q} = \begin{bmatrix} \Delta H \\ \Delta UH \end{bmatrix} \quad (65c)$$

All these quantities are necessary to calculate interface fluxes (such as the one given by Eq. (59)). However, the distribution of vegetation patches in vegetated flows is arbitrary, i.e. vegetated and free flow might alternate. This results in a jump in porosity at the interface between free flow and flow through vegetation. Since the flux in DIDANS equations depends not only on  $\mathbf{Q}$ , but also on the spatially variable porosity  $\phi = \phi(x)$ , which is a physical property of the flow domain, linearization of the homogeneous equation (49) results in an additional term.

*Discretisation of the term with spatially variable porosity*

The linearized form of Eq.(49) is:



$$\frac{\partial \mathbf{Q}}{\partial t} + \underbrace{\frac{\partial \mathbf{F}(\mathbf{Q}, \phi)}{\partial \mathbf{Q}}}_{\mathbf{A}(\mathbf{Q})} \frac{\partial \mathbf{Q}}{\partial x} + \underbrace{\frac{\partial \mathbf{F}(\mathbf{Q}, \phi)}{\partial \phi}}_{\mathbf{V}} \frac{\partial \phi}{\partial x} = 0 \quad (66)$$

$\Downarrow$  Roe                       $\Downarrow$  analogous to Hubbard and Navarro  
 $\tilde{\mathbf{A}}$                                        $\tilde{\mathbf{V}}$

In addition to Roe's Jacobian matrix, there is a vector  $\mathbf{V}$ , which is a partial derivative of the flux with respect to the spatially variable physical property of the flow domain. In Hubbard and Navarro [18] this is a variable channel width in the shallow water equations for the free flow, whereas in DIDANS equations for vegetated flow this is a variable porosity of the flow domain. The additional term takes into account the jump in porosity between the free and vegetated flows:

$$\Delta \phi = \phi_R - \phi_L \quad (67)$$

and, further to Roe's method, it is discretized using Roe's-average for the flow depth on that interface:

$$\tilde{\mathbf{V}} = \left[ 0 \quad -\frac{1}{2} g \tilde{h}^2 \right]^T \Delta \phi \quad (68)$$

The expression for the intercell flux at the edge  $i+1/2$  is now:

$$\mathbf{F}_{i+1/2} = \frac{1}{2} (\mathbf{F}_R + \mathbf{F}_L) - \frac{1}{2} \left( \tilde{\mathbf{R}} \tilde{\mathbf{\Lambda}} \tilde{\mathbf{R}}^{-1} \Delta \mathbf{Q} + \tilde{\mathbf{R}} \text{sign}(\mathbf{I}) \tilde{\mathbf{R}}^{-1} \tilde{\mathbf{V}} \right)_{i+1/2} \quad (69)$$

where

$$\text{sign}(\mathbf{I}) = \tilde{\mathbf{\Lambda}}^{-1} \left| \tilde{\mathbf{\Lambda}} \right| \quad (70)$$

\* \* \*

Boundary conditions for 1D DIDANS equations are calculated using the adapted method of characteristics. However, description of this method is beyond the scope of this lecture and the interested reader is referred to the paper [11].

#### 4 RESULTS OF TESTING OF ROE'S METHOD ADAPTED TO DIDANS EQUATIONS

In this section, several results of initial testing are presented to demonstrate the potential of the chosen numerical method. As already mentioned, the first step in testing the model is comparison of the numerical solution to the homogeneous equations to the analytical one for a control volume, if it exists, or to the numerical

solution of some other, reference scheme, which is proven to provide results of high accuracy. Analytical solution exists for the hypothetical case of steady flow in a horizontal bed channel partially occupied with vegetation when all resistance forces are neglected. The second test is comparison of the water surface profiles for non-uniform steady flow calculated with DIDANS and that for the equation of gradually varying flow obtained with the very fine space in a canal with the sloping bottom. Two cases are considered. One with vegetation occupying the upstream and the other with occupying the downstream half of the channel. In the third case, initial results for the case when the canal with the sloping bottom is occupied with vegetation along the full length are presented.

#### 4.1 TEST 1 – COMPARISON BETWEEN NUMERICAL AND ANALYTICAL SOLUTIONS FOR THE CONTROL VOLUME – STEADY FLOW IN A HORIZONTAL BED CHANNEL

A sketch of the 3 m long horizontal bed channel is presented in Figure 10. The channel is divided into two parts of equal length. One-half of the channel is uniformly occupied with rigid emergent cylinders and the other is empty. A solution to a problem in the vertical plane  $xOz$  is sought.

Four cases from Table 1 are analysed for the single value of porosity –  $\phi = 0,90$ . The initial depth in the channel is the same in all test cases and it equals 0,10 m. In cases with subcritical flow water is initially at rest, while in the supercritical flow the unit discharge in the channel is 0,12 m<sup>2</sup>/s. Boundary conditions in cases with subcritical flow are: unit discharge at the upstream boundary  $q_u \equiv (Uh)_u$  and the flow depth at the downstream end  $h_n$  (Figure 10). When the flow is supercritical, both boundary conditions are prescribed at the upstream boundary: unit discharge and the flow depth  $h_u$ . The value of the flow depth at the boundary is constant and it is the same in both flow regimes. It equals 0,1 m. The value of the unit discharge at the upstream boundary suddenly increases from the initial value to the prescribed value and it is kept constant. The analysed values of the unit discharge varied in the range between 0 and 0,25 m<sup>2</sup>/s. The simulation ended when the steady flow was reached.

The space and time steps in all simulations were  $\Delta x = 0,5$  m and  $\Delta t = 0,2$  s. Courant number did not exceed 0,5 in neither simulation.

Table 1. Analysed locations of vegetation and analysed flow regimes

Case No.	position of vegetation in a channel	flow regime
1	downstream half	subcritical
2	downstream half	supercritical
3	upstream half	subcritical
4	upstream half	supercritical

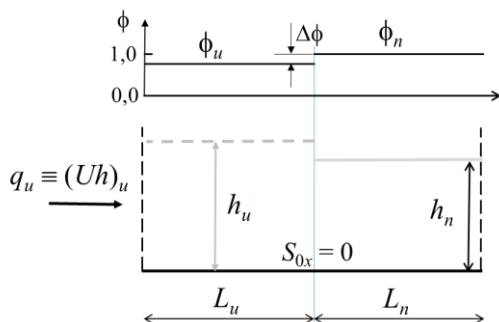


Figure 10. A sketch for the test cases for the adapted Roe's method

Simulation results are compared with the analytical solution for the steady flow (Figure 11). The analytical solution is a solution to the cubic equation:

$$\begin{aligned}
 A h_u^3 + B h_u + C &= 0 \\
 A &= 0,5 \phi_u^2 g \\
 B &= -\phi_u (\phi_n h_n U_n^2 + 0.5 \phi_n g h_n^2) \\
 C &= \phi_n^2 h_n^2 U_n^2
 \end{aligned} \tag{71}$$

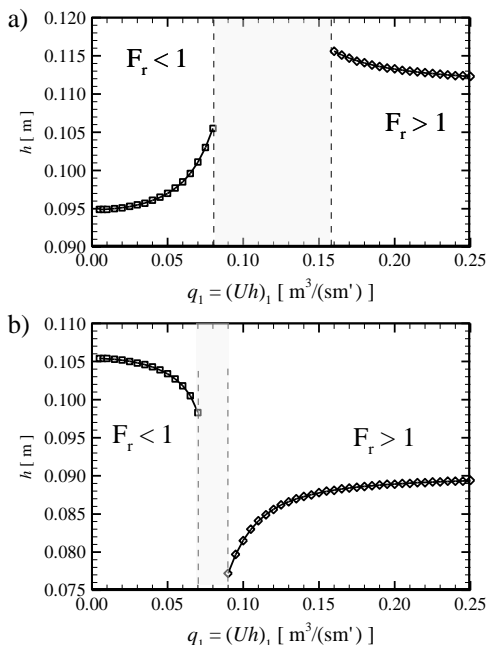


Figure 11. Comparison between numerical and analytical solutions for the cases when the vegetation occupies: a) downstream and b) upstream half of the channel. Analytical solution is presented with the solid line; numerical solutions are presented with symbols  $\square$  and  $\diamond$ . The light grey shaded area is the range where solution does not exist

Variables in expressions (71) are shown in Figure 10. Among the three solutions to the cubic equation (71), physically plausible one is taken, i.e. the one that corresponds to the flow regime under consideration. It is readily noticeable that numerical solutions fully comply with the analytical ones for both vegetation layouts and both flow regimes. Relative error is everywhere less than 5%. The blank space divides the regions with subcritical and supercritical flows. In this region solution to Eq. (71) does not exist.

#### 4.2 TEST 2 – SLOPING CHANNEL PARTIALLY FILLED WITH VEGETATION

Tests for non-homogeneous equations are performed for the sloping channel with  $S_{0x} = 0,001$ , friction and  $Dr$  neglected,  $\phi = 0,7$  and  $q = 0,025 \text{ m}^2/\text{s}$ . Both cases with vegetation occupying either downstream or upstream halves of the channel from Figure 10 are considered. Finite-volume size is  $\Delta x = 0,2 \text{ m}$  and the time step is  $\Delta t = 0,01 \text{ s}$ , giving again Courant number less than 0,5. Differences between DIDANS solution and that of the equation for the steady gradually varying flow with porosity (Figure 12) are less than 1%.

It is readily noticeable that the effects of vegetation presence are adverse along the upstream half of the channel when vegetation patch occupies its downstream and upstream halves. The presence of vegetation in the downstream half increases flow resistance and results in greater water depths along the upstream half of the channel. When the vegetation is located upstream, a decrease in water levels might be expected. It is interesting to notice that for the same downstream boundary condition, the water surface profile in the downstream half of the channel is the same regardless of the

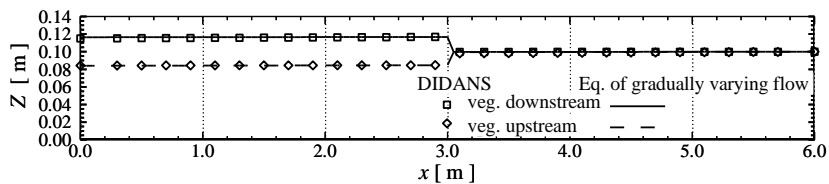


Figure 12. Comparison between numerical solutions to the non-homogeneous DIDANS equations (symbols) and solution to the equation of gradually varying flow with the porosity (lines) when  $S_{0x} = 0.001$ . Vegetation in the downstream (diamonds and the dashed line) and the upstream (squares and the solid line) half of the frictionless channel. Porosity is  $\phi = 0,7$ . Internal drag force is neglected.

location of the vegetation patch – downstream or upstream. Along the upstream stretch, water depths in the two water surface profiles differ by approximately 40%.

#### 4.3 TEST 3 – THE EFFECT OF VEGETATION DENSITY IN THE SLOPING CHANNEL

Finally, results of the initial tests of the effect of vegetation density in a sloping channel are presented for two bed slopes  $S_{0x} = \{0,001; 0,005\}$ . In this test, vegetation occupies the full length of the channel ( $L = 6,0 \text{ m}$ ). The space and time steps are  $\Delta x = 0,2 \text{ m}$  and  $\Delta t = 0,1 \text{ s}$ . Upstream and downstream boundary conditions were the same in all simulations. The upstream unit discharge was  $q = 0,040 \text{ m}^2/\text{s}$ , and the downstream water

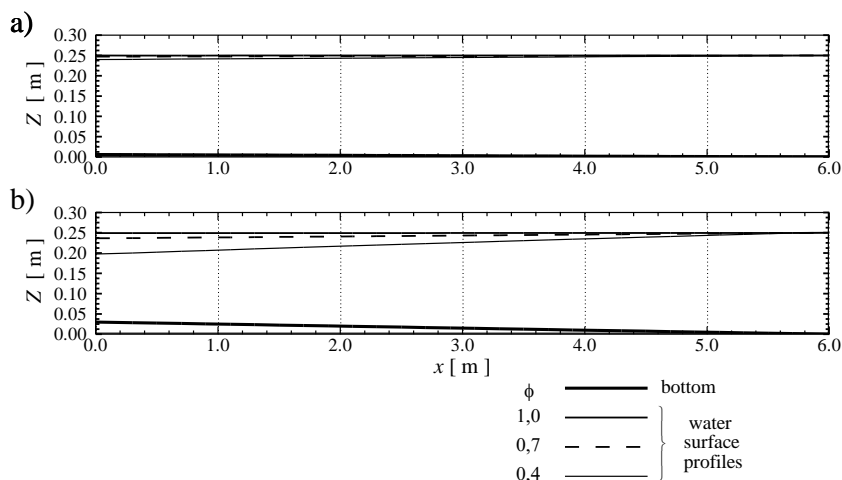


Figure 13. Effect of vegetation density (porosity  $\phi$ ) on the water surface profiles in a sloping channel: a)  $I_d = 0,001$  and b)  $I_d = 0,005$ . Flow is from left to right.

depth was  $h = 0,25$  m. Water surface profiles for two vegetation densities  $\phi = \{0,70; 0,40\}$  are compared to the case for the free flow ( $\phi = 1,00$ ) in Figure 13. The increase in vegetation density (decrease in porosity  $\phi$ ) for the given bed slope, causes decrease in water depths (water levels) when compared to the case with no vegetation in the channel (free flow  $\phi = 1,00$ ). The effect of vegetation presence becomes more prominent in channels with the larger bed slope. For  $S_{0x} = 0,001$  the water level at the upstream end of the channel decreases by approximately 1% for  $\phi = 0,70$  and 4% for  $\phi = 0,40$ , whereas for  $S_{0x} = 0,005$  these drops in water level reach 5% for  $\phi = 0,70$  and even 21% for  $\phi = 0,40$ .

## 5 CONCLUSIONS

The review of historical evolution of the double- averaging methodology undoubtedly indicate the advantages of using DANS over RANS (only time-averaged) equations in the analyses of spatially inhomogeneous flows. These advantages also extend to the triple averaged – DIDANS equations that were recently derived during the DoubleVeg project. They are listed below:

1. all forces that exist due to the presence of the solid phase – sediment grains, aquatic or riparian vegetation between or over which the water flows are explicitly encountered in the equations through the mathematically rigorous double averaging process. They are: the friction force between the water and the surface of roughness elements or the so-called viscous drag; form drag due to pressure variable pressure distribution around roughness elements; and the shear stress (force) due

to a departure of the time-averaged velocity at a point from the volume averaged value, or so-called form induced stress, and, additionally in DIDANS equations, shear stress due to departure of the double averaged velocity at the point in the vertical from the depth integrated value for the profile of the double averaged velocity in that vertical. In RANS equations these forces are introduced ad hoc and not by applying the principles of double averaging and transport and spatial-averaging theorems. The transport theorem shows that spatial averaging and time differentiation are not commutative if the averaging volume varies in time. The space-averaging theorem is introduced because space-averaging and differentiation operators are not commutative when the averaging volume depends on the position in space, i.e. on the three coordinates  $x_i$ ;

2. the possibility of clear and concise presentation of spatially heterogeneous flow using the double-averaged variables. Such a presentation allows one to examine global flow characteristics in the similar fashion the Reynolds averaging allows examination of the time-averaged flow;
3. the possibility of parametrisation of the terms in the double-averaged equations using the double-averaged values of the measured variables or the possibility of their decomposition to the components that describe the phenomena with the different levels of detail (for instance, decomposition of the instantaneous value of the momentum into four new terms). After parametrisation of all new averaged equations terms, the double averaged equations can be used for the development of numerical models.

Based on the above, it can be said that the double averaged Navier-Stokes equations are useful for [27]:

1. the development of numerical models,
2. planning of laboratory experiments and field campaigns on one hand, and numerical experiments, on the other,
3. the development of conceptual models for the new terms in equations that came out as a result of the double averaging or for their parametrisation,
4. the measurement data processing or for the processing of numerical simulation data and
5. the defining of models for the depth-integrated DANS equations, which describe flow in vegetated horizontal-bed open channels with an arbitrary distribution of vegetation patches, require adaptation of Roe's finite-volume method. Good agreement with an analytical solution indicates that one might expect good results for non-homogeneous equations.

The simulations conducted for a sloping bed channel partially filled with vegetation, with no friction and drag source terms added into the momentum equation, show a good match of the simulation results with the corresponding solution to the equation for gradually varied flow. The flow depths in the part of the channel occupied with vegetation decreased due to the presence of vegetation. However, its effect on the water depths in the free flow depends on its position in the channel. When the

vegetation occupies the downstream half of the channel, there is a significant increase in the upstream flow depths. On the other hand, when it is present in the upstream half of the channel, the flow depths along the downstream section are the same as when the vegetation was in that part of the channel.

The preliminary analysis of the effect of the vegetation density in the channel with the sloping bottom occupied with the vegetation along the channel length, again with no friction and drag forces added, reveals that with the increasing bottom slope, the vegetation presence has more prominent effects. Moreover, increasing vegetation density (reducing porosity) may significantly lower water levels at the upstream end of the channel (up to 20%).

## ACKNOWLEDGEMENTS

Although signed by a single author, this keynote lecture presents the results of the teamwork with Professor Dubravka Pokrajac, one of the world's leading experts in DAM. The author is indebted to Prof. Pokrajac for the acquisitions in hydraulics and computational hydraulics she gained as an undergraduate student at the Faculty of Civil Engineering in Belgrade. The pioneering work of the IAHR working group on DAM in open channel hydraulics, whose member was Prof. Pokrajac and her gift to present the most advanced mathematical work in an understandable, simple way resulting from her understanding of the underlying physics, aroused the author's interest in DAM. It was an inspiration for her to consider the possibility of extending the DAM to vegetated open-channel flows, especially to compound channel vegetated flows. The author expresses immense gratitude to Prof. Pokrajac for agreeing to collaborate on this research topic. This topic is of utmost importance for planning flood mitigation measures and will significantly impact the development of flood defence strategies in the coming decades.

## FUNDING

This research was supported by the Science Fund of the Republic of Serbia, Program DIASPORA, #GRANT No. 6466895, Acronym: DoubleVeg.

## REFERENCES

- [1] "data:image/jpeg;base64,/9j/," [Online].
- [2] J. Finnigan, "Turbulent transport in flexible plant canopies," in *In: The forest-atmosphere interactions*, e. B.A. Hutchinson and B.B. Hicks, Ed., D. Reidel Publishing Company, 1985, pp. 443-480.
- [3] J. Finnigan, "Turbulence in plant canopies," *Annu. Rev. Fluid. Mech.*, vol. 32, pp. 519-571, 2000.
- [4] G. Hajdin, *Mehanika fluida*, Beograd: Građevinski fakultet, 1982.
- [5] D. Pokrajac, "General shallow water equations (GSWEs)," *J. Hydraul. Res.*, vol. 61, no. 3, pp. 303-321, 2023.
- [6] [Online]. Available: [www.astro.cornell.edu](http://www.astro.cornell.edu).
- [7] E. Toro, *Riemann solvers and numerical methods for fluid dynamics: a practical introduction*, 2nd Ed. ed., Springer, 2009.
- [8] S. Whitaker, "Flow in porous media I: A theoretical derivation of Darcy's law," *Transport in Porous Media*, vol. 1, pp. 3-25, 1986.
- [9] S. Whitaker, *The method of volume averaging*, Dordrecht: Kluwer Academic Publishers, 1999.
- [10] R. LaVeque, *Finite Volume Methods For Hyperbolic Problems*, Cambridge University Press, 2002.
- [11] H. Barrios-Piña, H. Ramírez-León, C. Rodríguez-Cuevas and C. Couder-Castañeda, "Multilayer Numerical Modeling of Flows through Vegetation Using a Mixing-Length Turbulence Model," *Water*, vol. 6, pp. 2084-2103, 2014.
- [12] V. Nikora, "Hydrodynamics of aquatic ecosystems: an interface between ecology, biomechanics and environmental fluid mechanics," *River Res.Applic.*, vol. 26, p. 367–384, 2010.
- [13] J. Aberle and J. Järvelä, "Flow resistance of emergent rigid and flexible floodplain vegetation," *J. Hydraul. Res.*, vol. 51, no. 1, pp. 33-45, 2013.
- [14] Y. Bai and J. Duan, "Simulating unsteady flow and sediment transport in vegetated channel network," *J. Hydrol.*, vol. 515, pp. 90-102, 2014.
- [15] J. Bear, *Dynamics of Fluids in Porous Media*, Amsterdam: Elsevier, 1972.
- [16] A. Bello, D. Pokrajac and A. Leonardi, "Spatial Averaging over a variable volume and its implications for simulation of open channel flows over permeable beds," in *River Flow 2020: Proc. of the 10th conference on Fluvial Hydraulics*, Delft, the Netherland, 2020.
- [17] G. Caroppi, K. Västilä, P. Gualtieri, J. Järvelä, M. Giugni and P. M. Rowiński, "Comparison of flexible and rigid vegetation induced shear layers in partly vegetated channels," *Water Resour. Res.*, vol. 57, 2021.



- [18] M. Chatelain and P. S., "Open-channel flows through emergent rigid vegetation: Effects of bed roughness and shallowness on the flow structure and surface waves," *Physics of Fluids*, vol. 33, no. 10, 2021.
- [19] M. de Lemos and M. Pedras, "Recent mathematical models for turbulent flow in saturated rigid porous media," *J. Fluids Eng., ASME*, vol. 123, pp. 935-940, 2001.
- [20] D. Đorđević and D. Pokrajac, "Numeričko modeliranje linijskih otvorenih tokova sa promenljivim rasporedom vegetacije," *Vodoprivreda*, vol. 55, no. 325-326, pp. 143-153, 2023.
- [21] D. Đorđević and D. Pokrajac, "O Metodologiji dvostrukog osrednjavanja – pregled istorijskog razvoja i teorijske osnove," *Vodoprivreda*, vol. 52, no. 306-308, pp. 185-200, 2020.
- [22] L. Gimenez-Curto and M. Corniero Lera, "Oscillating turbulent flow over very rough surfaces," *J. Geophys. Res.*, vol. 101, no. C9, pp. 20,745-20,758, 1996.
- [23] J. Huang, X. Zhang and V. Chua, "Numerical modelling of longitudinal dispersion in tidal flows with submerged vegetation," *J. Hydraul. Res.*, vol. 53, no. 6, p. 728-746, 2015.
- [24] M. Hubbard and P. Garcia-Navarro, "Flux difference splitting and the balancing of source terms and flux gradients," *J. Comp. Phys.*, vol. 165, no. 1, pp. 89-125, 2000.
- [25] A. Leonardi, D. Pokrajac, F. Roman, F. Zanello and V. Armenio, "Surface and subsurface contributions to the build-up of forces on bed particles," *Journal of Fluid Mechanics*, vol. 85, no. 25, pp. 558-572, 2018.
- [26] M. Luhar, J. Rominger and H. Nepf, "Interaction between flow, transport and vegetation spatial structure," *Environ. Fluid Mech.*, vol. 8, pp. 423-439, 2008.
- [27] O. Musa, G. Huang, Z. Yua and Q. Li, "An improved Roe solver for high order reconstruction schemes," *Comp.&Fluids*, vol. 207, 2020.
- [28] H. Nepf and M. Ghisalberti, "Flow and transport in channels with submerged vegetation," *Acta Geophysica*, vol. 56, no. 3, pp. 753-777, 2008.
- [29] N. Nikora, V. Nikora and T. O'Donoghue, "Velocity profiles in vegetated open-channel flows: combined effects of multiple mechanisms," *J. Hydraul. Eng., ASCE*, vol. 139, no. 10, pp. 1021-1032, 2013.
- [30] V. Nikora, I. McEwan, S. McLean, S. Coleman, D. Pokrajac and R. Walters, "Double-averaging concept for rough-bed open-channel and overland flows: theoretical background," *J. Hydraul. Eng., ASCE*, vol. 133, no. 8, pp. 873-883, 2007.
- [31] V. Nikora, F. Ballio, S. Coleman and D. Pokrajac, "Spatially-averaged rough beds: definitions, averaging theorems and conservation equations," *J. Hydraul. Eng., ASCE*, vol. 139, no. 8, pp. 803-811, 2013.
- [32] V. Nikora, D. Goring, I. McEwan and G. Griffiths, "Spatially-averaged open-channel flow over a rough bed," *J. Hydraul. Eng., ASC*, vol. 127, no. 2, pp. 123-133, 2001.
- [33] D. Poggi, G. Katul and J. Albertson, "A note on the contribution of dispersive fluxes to momentum transfer within canopies," *Boundary-Layer Meteorology*, vol. 111, pp. 615-621, 2004.

- [34] D. Poggi, G. Katul and J. Albertson, "Momentum transfer and turbulent kinetic energy budgets within a dense canopy," *Boundary-Layer Meteorology*, vol. 111, pp. 589-614, 2004.
- [35] D. Pokrajac and M. de Lemos, "Spatial Averaging over a variable volume and its application to boundary-layer flows over permeable walls," *J. Hydraul. Eng., ASCE*, vol. 141, no. 4, 2015.
- [36] D. Pokrajac, I. McEwan and V. Nikora, "Spatially averaged turbulent stress and its partitioning," *Exp. Fluids*, vol. 45, pp. 73-83, 2008.
- [37] D. Pokrajac and C. Manes, "Velocity measurements of a free-surface turbulent flow penetrating a porous medium composed of uniform-size spheres," *Transport in Porous Media*, vol. 78, no. 3, pp. 367-383, 2009.
- [38] J. Qu and J. Yu, "A numerical modelling of flows in an open channel with emergent vegetation," *J. Hydraul. Res.*, vol. 59, no. 2, p. 250-262, 2021.
- [39] M. Raupach and R. Shaw, "Averaging procedures for flow within vegetation canopies," *Boundary-Layer Meteorology*, vol. 22, pp. 79-90, 1982.
- [40] M. Raupach, R. Antonia and S. Rajagopalan, "Rough-wall turbulent boundary layers," *Appl. Mech. Rev.*, vol. 44, no. 1, pp. 1-25, 1991.
- [41] F. Siniscalchi, V. I. Nikora and J. Aberle, "Plant patch hydrodynamics in streams: Mean flow, turbulence, and drag forces," *Water Resour. Res.*, vol. 48, 2012.
- [42] Y. Tanino and M. Nepf, "Laboratory investigation of mean drag in random array of rigid, emergent cylinders," *J. Hydraul. Eng., ASCE*, vol. 134, no. 1, pp. 34-41, 2008.
- [43] Y. Tanino and M. Nepf, "Lateral dispersion in random cylinder arrays at high Reynolds number," *J. Fluid Mech.*, vol. 600, pp. 339-371, 2008.
- [44] S. H. Truong and W. S. J. Uijttewaal, "Transverse momentum exchange induced by large coherent structures in a vegetated compound channel," *Water Resour. Res.*, vol. 55, p. 589-612, 2019.
- [45] M. Wang, E. Avital, Q. Chen, J. Williams, S. Mi and Q. Xie, "A numerical study on suspended sediment transport in a partially vegetated channel flow," *J. Hydrol.*, vol. 599, 2021.
- [46] B. White and H. Nepf, "Shear instability and coherent structures in shallow flow adjacent to a porous layer," *J. Fluid Mech.*, vol. 593, pp. 1-32, 2007.
- [47] N. Wilson and R. Shaw, "A higher order closure model for canopy flow," *J. Appl. Meteorology*, vol. 16, pp. 1197-1205, 1977.